NASA TECHNICAL NOTE

NASA TN D-8376

FREE-VIBRATION CHARACTERISTICS OF A LARGE SPLIT-BLANKET SOLAR ARRAY IN A 1-g FIELD

Francis J. Shaker

Lewis Research Center
Cleveland, Ohio 44135

NATIONAL AERONAUTICS AND SPACE ADMINISTRATION • WASHINGTON, D. C. • DECEMBER 1976

1. Report No.	2. Government Accession No.	3. Recipient's Catalog No.
NASA TN D-8376		

4. Title and Subtitle: FREE-VIBRATION CHARACTERISTICS OF A LARGE SPLIT-BLANKET SOLAR ARRAY IN A 1-g FIELD

5. Report Date: December 1976

6. Performing Organization Code:

7. Author(s): Francis J. Shaker

8. Performing Organization Report No.: E-8827

9. Performing Organization Name and Address:
Lewis Research Center
National Aeronautics and Space Administration
Cleveland, Ohio 44135

10. Work Unit No.: 506-22

11. Contract or Grant No.:

12. Sponsoring Agency Name and Address:
National Aeronautics and Space Administration
Washington, D.C. 20546

13. Type of Report and Period Covered: Technical Note

14. Sponsoring Agency Code:

15. Supplementary Notes:

16. Abstract

Two methods for studying the free-vibration characteristics of a large split-blanket solar array in both a 0-g and a 1-g cantilevered configuration are presented. The 0-g configuration corresponds to an in-orbit configuration of the array; the 1-g configuration is a typical ground-test configuration. The first method applies the equations of continuum mechanics to determine the mode shapes and frequencies of the array; the second method uses the Rayleigh-Ritz approach. In the Rayleigh-Ritz method the array displacements are represented by string modes and cantilevered beam modes. The results of this investigation are summarized by a series of graphs illustrating the effects of various array parameters on the mode shapes and frequencies of the system. The results of the two methods are also compared in tabular form.

17. Key Words (Suggested by Author(s))	18. Distribution Statement
Solar array Dynamic structural analysis	Unclassified - unlimited STAR Category 39

19. Security Classif. (of this report)	20. Security Classif. (of this page)	21. No. of Pages	22. Price*
Unclassified	Unclassified	62	$4.50

* For sale by the National Technical Information Service, Springfield, Virginia 22161

CONTENTS

FREE-VIBRATION CHARACTERISTICS OF A LARGE SPLIT-BLANKET SOLAR ARRAY IN A 1-g FIELD

by Francis J. Shaker

Lewis Research Center

SUMMARY

Two methods for studying the free-vibration characteristics of a large split-blanket solar array in both a 0-g and a 1-g cantilevered configuration are presented. The 0-g configuration corresponds to an in-orbit configuration of the array; the 1-g configuration is a typical ground-test configuration. The first method applies the equations of continuum mechanics to determine the mode shapes and frequencies of the array; the second method uses the Rayleigh-Ritz approach. In the Rayleigh-Ritz method the array displacements are represented by string modes and cantilevered beam modes. The results of this investigation are summarized by a series of graphs illustrating the effects of various array parameters on the mode shapes and frequencies of the system. The results of the two methods are also compared in tabular form.

INTRODUCTION

To predict the dynamic behavior of a spacecraft with large, flexible solar arrays, it is first necessary to describe the structural dynamic characteristics of the array. These characteristics can be determined once the cantilevered modes and frequencies of the flexible solar array in a 0-g environment are known (refs. 1 and 2).

In addition to the 0-g modes and frequencies, it sometimes becomes necessary to predict the dynamic behavior of the array while it is suspended vertically in a 1-g field. This is the usual ground-test configuration for studying the dynamic behavior of large solar arrays (refs. 3 and 4). In this configuration the blanket weight has a significant effect on the dynamics of the array and must be included when predicting the behavior of the system.

The cantilevered modes and frequencies of a split-blanket solar array have been studied by several investigators in recent years. As shown in figure 1 a split-blanket solar array consists of a central support boom, a two-piece blanket substrate with solar

cells mounted on one side, and a leading-edge member that transfers a tension load to the blanket from the boom. For this type of array the boom centerline lies in the plane of the blanket. In reference 5 the cantilevered modes and frequencies of a split-blanket array in a 0-g field were investigated by solving the differential equations governing the motion. This method results in transcendental equations that can be solved numerically for the frequencies. In reference 6 the finite element method was used to find the cantilevered modes and frequencies of this type of array. Beam-column elements were used to describe the array boom, and membrane elements to describe the blanket. Seventeen and 26 degrees of freedom were used to determine the fundamental antisymmetric (torsional) and symmetric (bending) modes and frequencies, respectively. Using the finite element method to determine higher modes and frequencies would require a large number of degrees of freedom to obtain the same accuracy. In reference 7 the modes and frequencies of a solar array in which the blanket is offset from the centerline of the boom are investigated by using a Rayleigh-Ritz approach. The assumed modes used to construct the Rayleigh-Ritz solutions were polynomials to the fourth order.

The purpose of the present report is twofold. First, it presents the exact solution for the modes and frequencies of a split-blanket solar array in a 1-g field and compares this solution with a Rayleigh-Ritz approximate solution. Second, by using these solutions it investigates the effects of various solar array parameters (mass, blanket tension, boom stiffness, etc.) on the modes and frequencies of large solar arrays in both a 0-g and a 1-g configuration. In developing the Rayleigh-Ritz solution, cantilevered beam modes and string modes are used to represent the boom and blanket displacements, respectively. Using these modes will ensure convergence for a relatively small number of modes or degrees of freedom. The effects of solar array parameters on the modes and frequencies are illustrated by a series of graphs, and comparisons between exact and approximate solutions are shown in tabular form.

THEORETICAL DEVELOPMENT OF NORMAL MODES AND FREQUENCIES OF LARGE SPLIT-BLANKET SOLAR ARRAY

Continuum Mechanics Approach

Basic assumptions. - For purposes of analysis a large split-blanket solar array is idealized, as shown in figure 1. This figure shows the array consisting of three components: a center boom that supports the array; a membrane substrate with solar cells attached to one side (hereinafter referred to as the blanket); and a bar at the tip of the boom that transfers a tension load P from the boom to the substrate. The displacements of the boom and blanket, normal to the plane of the blanket, are denoted by $V(x,t)$

and $W(x,y,t)$, respectively. In developing the equations of motion for the array the following assumptions were made:

(1) The bending stiffness of the blanket, normal to its plane, is negligible so that the blanket behaves like a membrane in this direction.

(2) The tension distribution is uniform across the width of the blanket (i.e., the tip piece is perfectly rigid).

(3) Displacements are small, so that small-displacement theory is valid.

(4) Boom weight is negligible and the shear center coincides with the neutral axis of the boom.

Based on these assumptions the equations describing the motion of the array were developed. (All symbols are defined in appendix A.)

Equations of motion. - The forces acting on an element of the blanket displaced an amount $W(x,y,t)$ from its static equilibrium configuration are shown in figure 2(a). Applying Newton's second law of motion to this element yields the following equation:

$$T \frac{\partial}{\partial x}\left(\frac{\partial W}{\partial x}\right) + \frac{\partial W}{\partial x} \frac{dT}{dx} = \frac{\rho_m}{b} \frac{\partial^2 W}{\partial t^2} \tag{1}$$

where b is the blanket width and ρ_m is the mass per unit length of blanket. It can readily be seen that an alternative form of equation (1) is given by

$$\frac{\partial}{\partial x}\left(T \frac{\partial W}{\partial x}\right) = \frac{\rho_m}{b} \frac{\partial^2 W}{\partial t^2} \tag{2}$$

Now for a blanket hanging vertically the tension at any point x will be a superposition of the preload P transferred to the blanket from the boom and the weight of the blanket below the point x. That is,

$$T(x) = \frac{P}{b}\left(1 + \frac{W_m}{P} - \frac{\rho_m g}{P} x\right) \tag{3}$$

where W_m is the total blanket weight. In view of equation (3), equation (1) is transformed by making the following change of variables:

$$\zeta^2 = \frac{b}{P} T(x) = 1 + \frac{W_m}{P} - \frac{\rho_m g}{P} x \tag{4}$$

From equations (1) and (4) then

$$\frac{\partial^2 W}{\partial \zeta^2} + \frac{1}{\zeta}\frac{\partial W}{\partial \zeta} - \frac{4\rho_m \ell^2}{P}\left(\frac{P}{W_m}\right)^2 \frac{\partial^2 W}{\partial t^2} = 0 \tag{5}$$

Equation (5) represents the desired form for the equation of motion of the blanket.

The equation of motion of the boom can be developed by applying Newton's second law of motion to the beam element shown in figure 2(b) and by using the following force-displacement relations from elementary beam theory:

$$Q(x) = -EI\left(\frac{\partial^3 V}{\partial x^3} + \frac{P}{EI}\frac{\partial V}{\partial x}\right) \tag{6a}$$

$$M_y(x) = EI\frac{\partial^2 V}{\partial x^2} \tag{6b}$$

In this manner it can be shown (ref. 8) that the equation governing the bending motion of the boom is given by

$$\frac{\partial^4 V}{\partial x^4} + \frac{P}{EI}\frac{\partial^2 V}{\partial x^2} + \frac{\rho_b}{EI}\frac{\partial^2 V}{\partial t^2} = 0 \tag{7}$$

In addition to the bending motion described by equation (7), the boom can also experience a rotational motion about its centerline. The equation governing this motion is developed in numerous texts on vibration theory (e.g., ref. 9) and is given by

$$\frac{\partial^2 \theta}{\partial x^2} - \frac{I_b}{JG}\frac{\partial^2 \theta}{\partial t^2} = 0 \tag{8}$$

where θ is the rotational angle of the boom cross section, I_b is the mass polar moment of inertia per unit length, and JG is the torsional stiffness of the boom. The relation between the torsional moment M_x and the angular rotation θ used in developing equation (8) is

$$M_x(x) = JG\frac{\partial \theta}{\partial x} \tag{9}$$

Equations (6) to (9) represent the required relations for the boom.

The final set of equations are the equations of motion for the tip piece. The forces acting on the tip piece are shown in figure 3. Applying Newton's second law of motion for forces in the z-direction and moments about an axis parallel to the x-axis and passing through the center of gravity of the tip piece yields the following two equations:

$$Q(\ell, t) + \int_{-b/2}^{b/2} \frac{P}{b} \frac{\partial W(\ell, y, t)}{\partial x} dy + M_{tp} \frac{\partial^2 V(\ell, t)}{\partial t^2} = 0 \tag{10}$$

$$M_x(\ell, t) + \int_{-b/2}^{b/2} \frac{P}{b} y \frac{\partial W(\ell, y, t)}{\partial x} dx + I_{tp} \frac{d^2\alpha}{dt^2} = 0 \tag{11}$$

where M_{tp} is the mass of the tip piece and I_{tp} is the mass moment of inertia about its center of gravity. Eliminating the force and moment in equations (10) and (11) by using equations (6a) and (9) and changing the variables in W from x to ζ by using equation (4) transforms equations (10) and (11) into the following equations:

$$\frac{\partial^3 V(\ell, t)}{\partial x^3} + \frac{P}{EI} \frac{\partial V(\ell, t)}{\partial x} + \frac{1}{2\ell b} \left(\frac{P}{EI}\right)\left(\frac{W_m}{P}\right) \int_{-b/2}^{b/2} \frac{\partial W(1, y, t)}{\partial \zeta} dy - \frac{M_{tp}}{EI} \frac{\partial^2 V(\ell, t)}{\partial t^2} = 0 \tag{12}$$

$$\frac{\partial \theta(\ell, t)}{\partial x} - \frac{1}{2\ell b} \left(\frac{P}{JG}\right)\left(\frac{W_m}{P}\right) \int_{-b/2}^{b/2} y \frac{\partial W(1, y, t)}{\partial \zeta} dy + \frac{I_{tp}}{JG} \frac{d^2\alpha}{dt^2} = 0 \tag{13}$$

Equations (12) and (13) represent the final form of the equations of motion of the tip piece. These equations together with equations (5), (7), and (8) represent the motion equations for the complete solar array. The displacement variables in these equations must satisfy certain boundary and compatibility relations. These conditions are given next.

Boundary conditions and compatibility relations. - At the fixed end of the array the displacements and rotations of the array elements are all zero. At this end, x = 0 and it follows from equation (4) that $\zeta = \zeta_0 = \sqrt{1 + (W_m/P)}$. Thus, the boundary conditions at the fixed end will be as follows:

$$\left.\begin{aligned} V(0,t) &= 0 \\ \frac{\partial V}{\partial x}(0,t) &= 0 \\ \theta(0,t) &= 0 \\ W(\zeta_0,y,t) &= 0 \end{aligned}\right\} \tag{14}$$

At the free end of the array the displacements and rotations of the components must be compatible. At this end $x = \ell$; and from equation (4), $\zeta = 1$. In addition, the moment at the tip of the boom (given by eq. (6b)) is zero. Thus, the boundary and compatibility relations at the free end are as follows:

$$\left.\begin{aligned} \theta(\ell,t) &= \alpha \\ W(1,0,t) &= V(\ell,t) \\ W(1,y,t) &= W(1,0,t) + y\alpha \\ \frac{\partial^2 V}{\partial x^2}(\ell,t) &= 0 \end{aligned}\right\} \tag{15}$$

Equations (12) to (15) represent the complete set of relations that must be satisfied by the solutions to equations (5), (7), and (8).

Separation of variables. - The first step in the solution of the motion equations is to eliminate the y and t variables by assuming a harmonic solution of the following form:

$$\left.\begin{aligned} V(x,t) &= v(x)e^{i\omega t} \\ W(\zeta,y,t) &= [w(\zeta) + y\varphi(\zeta)]e^{i\omega t} \\ \theta(x,t) &= \theta(x)e^{i\omega t} \end{aligned}\right\} \tag{16}$$

From equations (16) and (5), (7), (8), and (12) to (15), two independent sets of equations and corresponding boundary conditions are obtained. These equations can be nondimensionalized by making the following substitutions:

$$\left.\begin{aligned}
&\bar{x} = \frac{x}{l},\ \bar{v} = \frac{v}{l},\ \bar{w} = \frac{w}{l},\ \bar{P} = \frac{P}{W_m},\ \bar{\beta}_t^2 = \frac{M_w l}{P}\omega^2, \\
&\bar{k}^2 = \frac{Pl^2}{EI},\ \bar{k}_t^2 = \frac{Pb^2}{JG},\ \bar{\beta}^4 = \frac{M_b l^3}{EI}\omega^2,\ \bar{M}_m = \frac{M_m}{M_b}, \\
&\bar{M}_{tp} = \frac{M_{tp}}{M_b},\ \bar{b} = \frac{b}{l},\ \bar{I}_{tp} = \frac{I_{tp}}{M_m b^2},\ \bar{I}_b = \frac{I_b}{\rho_m b^2} \\
&\kappa_1^2 = \frac{\bar{M}_m \bar{P}^2}{\bar{k}^2}
\end{aligned}\right\} \tag{17}$$

where M_m is the total mass of the blanket and M_b is the total mass of the beam. The first nondimensional set of equations is designated as the bending equations and is given by

$$\frac{d^2\bar{w}}{d\zeta^2} + \frac{1}{\zeta}\frac{d\bar{w}}{d\zeta} + 4\kappa_1^2\bar{\beta}^4\bar{w} = 0 \tag{18a}$$

$$\frac{d^4\bar{v}}{d\bar{x}^4} + \bar{k}^2\frac{d^2\bar{v}}{d\bar{x}^2} - \bar{\beta}^4\bar{v} = 0 \tag{18b}$$

$$\frac{d^3\bar{v}(1)}{d\bar{x}^3} + \bar{k}^2\frac{d\bar{v}(1)}{d\bar{x}} + \frac{1}{2}\frac{\bar{k}^2}{\bar{P}}\frac{d\bar{w}(1)}{d\zeta} + \bar{M}_{tp}\bar{\beta}^4\bar{v}(1) = 0 \tag{19}$$

with boundary conditions

$$\bar{v}(0) = 0 \tag{20a}$$

$$\frac{d\bar{v}(0)}{d\bar{x}} = 0 \tag{20b}$$

$$\bar{w}(\zeta_0) = 0 \tag{20c}$$

$$\left.\begin{aligned} \bar{w}(1) &= \bar{v}(1) \\ \frac{d^2\bar{v}(1)}{d\bar{x}^2} &= 0 \end{aligned}\right\} \tag{21}$$

The second set of equations is called the torsion equations and is given by

$$\frac{d^2\varphi}{d\zeta^2} + \frac{1}{\zeta}\frac{d\varphi}{d\zeta} + 4\bar{\beta}_t^2\bar{P}^2\varphi = 0 \tag{22a}$$

$$\frac{d^2\theta}{d\bar{x}^2} + \bar{I}_b\bar{k}_t^2\bar{\beta}_t^2\theta = 0 \tag{22b}$$

$$\frac{d\theta(1)}{d\bar{x}} - \frac{1}{24}\frac{\bar{k}_t^2}{\bar{P}}\frac{d\varphi(1)}{d\zeta} - \bar{I}_{tp}\bar{k}_t^2\bar{\beta}_t^2\theta(1) = 0 \tag{23}$$

with boundary conditions

$$\theta(0) = 0 \tag{24a}$$

$$\varphi(\zeta_0) = 0 \tag{24b}$$

$$\theta(1) = \varphi(1) \tag{24c}$$

Equations (18) and (19) and boundary conditions (20) and (21) define the bending or symmetric motions of the array in which the blanket displacements are independent of y. This type of displacement field is illustrated in figure 4(a). Similarly, equations (22) and (23) and boundary conditions (24) define the torsional or antisymmetric motions of the array, in which the blanket displacements vary linearly with y. Figure 4(b) illustrates this type of displacement field.

Solution to bending equations. - To obtain a solution to the bending equations, a solution to equations (18) that satisfies equations (19) to (21) must be determined. Now, equation (18a) is Bessel's equation of zero order, and its solution satisfying boundary condition (20c) is (ref. 10)

$$\bar{w}(\zeta) = C\left[Y_0(2\kappa_1\bar{\beta}^2\zeta_0)J_0(2\kappa_1\bar{\beta}^2\zeta) - J_0(2\kappa_1\bar{\beta}^2\zeta_0)Y_0(2\kappa_1\bar{\beta}^2\zeta)\right] \tag{25}$$

where J_0 and Y_0 are Bessel functions of the first and second kind, respectively, of zero order and C is an unknown constant. Also, it can be shown by direct substitution that the solution to equation (18b), satisfying boundary conditions (20a) and (20b), is

$$\bar{v}(x) = A(\alpha_2 \cosh \alpha_1 \bar{x} - \alpha_2 \cos \alpha_2 \bar{x}) + B(\alpha_2 \sinh \alpha_1 \bar{x} - \alpha_1 \sin \alpha_2 \bar{x}) \tag{26}$$

where

$$\left.\begin{aligned} \alpha_1 &= \left(-\frac{\bar{k}^2}{2} + \sqrt{\frac{\bar{k}^4}{4} + \bar{\beta}^4}\right)^{1/2} \\ \alpha_2 &= \left(\frac{\bar{k}^2}{2} + \sqrt{\frac{\bar{k}^4}{4} + \bar{\beta}^4}\right)^{1/2} \end{aligned}\right\} \tag{27}$$

and A and B are unknown constants. Now equations (25) and (26) contain three unknown constants that can be evaluated from the three remaining conditions given by equations (19) and (21). Utilizing equations (25) and (26) changes equations (21) to

$$A(\alpha_2 \cosh \alpha_1 - \alpha_2 \cos \alpha_2) + B(\alpha_2 \sinh \alpha_1 - \alpha_1 \sin \alpha_2) - CF_1(\bar{\beta}) = 0 \tag{28}$$

$$A\left(\alpha_1^2 \cosh \alpha_1 + \alpha_2^2 \cos \alpha_2\right) + B\left(\alpha_1^2 \sinh \alpha_1 + \alpha_1 \alpha_2 \sin \alpha_2\right) = 0 \tag{29}$$

where

$$F_1(\bar{\beta}) = Y_0\left(2\kappa_1 \bar{\beta}^2 \zeta_0\right) J_0\left(2\kappa_1 \bar{\beta}^2\right) - J_0\left(2\kappa_1 \bar{\beta}^2 \zeta_0\right) Y_0\left(2\kappa_1 \bar{\beta}^2\right) \tag{30}$$

The third equation is obtained from equation (19) by using equations (25) and (26). After some manipulation with Bessel functions, this equation can be written as

$$\begin{aligned} A\left[\left(\alpha_2^2 \sinh \alpha_1 - \alpha_1 \alpha_2 \sin \alpha_2\right) + \bar{M}_{tp} \bar{\beta}^2 (\alpha_2 \cosh \alpha_1 - \alpha_2 \cos \alpha_2)\right] \\ + B\left[\left(\alpha_2^2 \cosh \alpha_1 + \alpha_1^2 \cos \alpha_1\right) + \bar{M}_{tp} \bar{\beta}^2 (\alpha_2 \sinh \alpha_1 - \alpha_1 \sin \alpha_2)\right] \\ - C\left[\frac{\bar{k}^2}{P\bar{\beta}^2} F_2(\bar{\beta})\right] = 0 \end{aligned} \tag{31}$$

where $F_2(\bar{\beta})$ is defined in terms of Bessel functions of the zero and first orders as

$$F_2(\bar{\beta}) = \frac{1}{J_0\left(2\kappa_1\bar{\beta}^2\right)}\left[\kappa_1\bar{\beta}^2 J_1\left(2\kappa_1\bar{\beta}^2\right)F_1(\bar{\beta}) + \frac{1}{\pi}J_0\left(2\kappa_1\bar{\beta}^2\zeta_0\right)\right] \tag{32}$$

Equations (28), (29), and (31) represent three equations in three unknowns, A, B, and and C. For a nontrivial solution the determinant of the coefficients of the unknowns must be zero. Expanding this determinant and simplifying yield the following equation:

$$\left[F_1(\bar{\beta})\bar{M}_{tp}\bar{\beta}^4 - \frac{\bar{k}^2}{\bar{P}}F_2(\bar{\beta})\right]\left[\left(\alpha_1^2 + \alpha_2^2\right)(\alpha_2 \sinh \alpha_1 \cos \alpha_2 - \alpha_1 \cosh \alpha_1 \sin \alpha_2)\right]$$

$$+ F_1(\bar{\beta})\left[2\bar{\beta}^6 + \bar{\beta}^2(2\bar{\beta}^4 + \bar{k}^4)\cosh \alpha_1 \cos \alpha_2 - \bar{\beta}^4\bar{k}^2 \sinh \alpha_1 \sin \alpha_2\right] = 0 \tag{33}$$

Equation (33) is the characteristic equation for the bending vibrational frequencies of a split-blanket solar array in a 1-g field. When the mass parameters $\bar{M}_{tp}$ and $\bar{M}_b$ and the load parameters $\bar{P}$ and $\bar{k}$ are specified, the frequency parameters $\bar{\beta}$ can be determined numerically. Note that equation (33) is valid, provided the boom does not buckle. That is, the load P must be less than the critical buckling load of the array. Development of this critical buckling load is presented in appendix A. For P equal to P_{cr}, it can be shown that equation (33) yields $\bar{\beta} = 0$.

Solution to torsion equations. - The torsion equations can be solved in a manner similar to that used for the bending equations. It can be verified by direct substitution that the solution to equations (22) satisfying the boundary conditions (24a) and (24b) is given by

$$\left.\begin{aligned} \theta &= A_1 \sin\left(\bar{I}_b^{1/2}\bar{k}_t\bar{\beta}_t\bar{x}\right) \\ \varphi &= B_1\left[Y_0(2\kappa_2\zeta_0)J_0(2\kappa_2\zeta) - J_0(2\kappa_2\zeta_0)Y_0(2\kappa_2\zeta)\right] \end{aligned}\right\} \tag{34}$$

where $\kappa_2 = \bar{\beta}_t\bar{P}$. The constants A_1 and B_1 are such that conditions given by equations (23) and (24c) must be satisfied. By using equations (34) these equations become

$$\left.\begin{aligned} A_1 \sin\left(\bar{I}_b^{1/2}\bar{k}_t\bar{\beta}_t\right) - B_1F_3(\bar{\beta}_t) &= 0 \\ A_1\left[\bar{I}_b^{1/2}\bar{k}_t\bar{\beta}_t \cos\left(\bar{I}_b^{1/2}\bar{k}_t\bar{\beta}_t\right) - \bar{I}_{tp}\bar{k}_t^2\bar{\beta}_t^2 \sin\left(\bar{I}_b^{1/2}\bar{k}_t\bar{\beta}_t\right)\right] + B_1\frac{\bar{k}_t^2}{\bar{P}}F_4(\bar{\beta}_t) &= 0 \end{aligned}\right\} \tag{35}$$

where

$$\left.\begin{aligned} F_3(\bar{\beta}_t) &= Y_0(2\kappa_2\zeta_0)J_0(2\kappa_2) - J_0(2\kappa_2\zeta_0)Y_0(2\kappa_2) \\ F_4(\bar{\beta}_t) &= \frac{1}{J_0(2\kappa_2)}\left[\kappa_2 J_1(2\kappa_2)F_3(\bar{\beta}_t) + \frac{1}{\pi}J_0(2\kappa_2\zeta)\right] \end{aligned}\right\} \tag{36}$$

Equating the determinant of the coefficients of the unknowns A_1 and B_1 in equations (35) to zero yields

$$\frac{1}{12\kappa_2}F_4(\bar{\beta}_t)\sin\left(\bar{I}_b^{1/2}\bar{k}_t\bar{\beta}_t\right) + F_3(\bar{\beta}_t)\left[\frac{\bar{I}_b^{1/2}}{\bar{k}_t}\cos\left(\bar{I}_b^{1/2}\bar{k}_t\bar{\beta}_t\right) - \bar{I}_{tp}\bar{\beta}_t\sin\left(\bar{I}_b^{1/2}\bar{k}_t\bar{\beta}_t\right)\right] = 0 \tag{37}$$

Equation (37) is the characteristic equation for the torsional frequencies of the array in a 1-g field. Once the inertia parameters $\bar{I}_b$ and $\bar{I}_{tp}$ and the load parameters $\bar{k}_t$ and $\bar{P}$ are specified, the frequency parameters β_t can be found by solving this equation numerically. If the mass of the boom is negligible such that $\sin\left(\bar{I}_b^{1/2}\bar{k}_t\bar{\beta}_t\right) \approx \bar{I}_b^{1/2}\bar{k}_t\bar{\beta}_t$ and $\cos\left(\bar{I}_b^{1/2}\bar{k}_t\bar{\beta}_t\right) \approx 1$, then equation (37) simplifies somewhat to

$$\frac{F_4(\bar{\beta}_t)}{\kappa_2} + 12F_3(\bar{\beta}_t)\left(\frac{1}{\bar{k}_t^2\bar{\beta}_t} - \bar{I}_{tp}\bar{\beta}_t\right) = 0 \tag{38}$$

Equation (38) is applicable to current large solar array designs.

Degenerate case - 0-g configuration. - For the case of a solar array in a 0-g field (i.e., an in-orbit configuration) the characteristic equations for the bending and torsional frequencies can be determined from equations (33) and (38) by taking the limit of the functions in these equations as the blanket weight W_m approaches zero. It is shown in appendix B that as W_m approaches 0 the following relations hold:

$$F_1(\bar{\beta}) = \frac{1}{\pi\kappa_1\bar{\beta}^2\zeta_0}\sin\alpha_3 \tag{39a}$$

$$F_2(\bar{\beta}) = \frac{\alpha_3\bar{P}}{\pi\kappa_1\bar{\beta}^2\zeta_0^{1/2}}\cos\alpha_3 \tag{39b}$$

$$F_3(\bar{\beta}_t) = \frac{1}{\pi \kappa_2 \zeta_0} \sin \bar{\beta}_t \tag{40a}$$

$$F_4(\bar{\beta}_t) = \frac{1}{\pi \zeta_0^{1/2}} \cos \bar{\beta}_t \tag{40b}$$

where

$$\alpha_3 = \frac{\bar{M}_m^{1/2}}{\bar{k}} \bar{\beta}^2 \tag{41}$$

Substituting equations (39) into equation (33) yields the following characteristic equation for the bending frequencies of the array in a 0-g configuration:

$$\left(\bar{M}_{tp}\bar{\beta}^4 \sin \alpha_3 - \bar{k}^2 \alpha_3 \cos \alpha_3\right)\left[\left(\alpha_1^2 + \alpha_2^2\right)(\alpha_2 \sinh \alpha_1 \cos \alpha_2 - \alpha_1 \cosh \alpha_1 \sin \alpha_2)\right]$$

$$+ \sin \alpha_3 \left[2\bar{\beta}^6 + \bar{\beta}^2(2\bar{\beta}^4 + \bar{k}^4)\cosh \alpha_1 \cos \alpha_2 - \bar{\beta}^4 \bar{k}^2 \sinh \alpha_1 \sin \alpha_2\right] = 0 \tag{42}$$

Similarly, the characteristic equation for torsion is obtained by substituting equations (40) into equation (38), which yields

$$\cos \bar{\beta}_t + 12\left(\frac{1}{\bar{k}_t^2 \bar{\beta}_t} - \bar{I}_{tp}\bar{\beta}_t\right) \sin \bar{\beta}_t = 0 \tag{43}$$

It can be shown that equations (42) and (43) are analogous to the frequency equations in reference 3, which were developed in a straightforward manner for the 0-g configuration.

Mode shapes and orthogonality conditions. - To determine the bending mode shapes of the solar array, assume that the frequency parameter for the n^{th} mode $\bar{\beta}_n$ is known. Corresponding to $\bar{\beta}_n$ there will be an α_{1n} and α_{2n}. Starting with equations (25) and (26) the boom and blanket displacements in the n^{th} mode will be

$$\bar{v}_n(\bar{x}) = A_n(\alpha_{2n} \cosh \alpha_{1n} \bar{x} - \alpha_{2n} \cos \alpha_{2n}\bar{x}) + B_n(\alpha_{2n} \sinh \alpha_{1n}\bar{x} - \alpha_{1n} \sin \alpha_{2n}\bar{x}) \tag{44}$$

$$\bar{w}_n(\xi) = C_n\left[Y_0\left(2\kappa_1\xi_0\bar{\beta}_n^2\right)J_0\left(2\kappa_1\bar{\beta}_n^2\xi\right) - J_0\left(2\kappa_1\bar{\beta}_n^2\xi_0\right)Y_0\left(2\kappa_1\bar{\beta}_n^2\xi\right)\right] \tag{45}$$

The mode shapes can be determined from equations (44) and (45) by expressing B_n and C_n in terms of A_n, using the boundary conditions expressed by equations (28) and (29). From these equations then

$$B_n = \frac{-\left(\alpha_{1n}^2 \cosh \alpha_{1n} + \alpha_{2n}^2 \cos \alpha_{2n}\right)}{\alpha_{1n}^2 \sinh \alpha_{1n} + \alpha_{1n}\alpha_{2n} \sin \alpha_{2n}} A_n \tag{46}$$

$$C_n = \frac{1}{F_1(\bar{\beta}_n)}\left[\alpha_{2n}(\cosh \alpha_{1n} - \cos \alpha_{2n}) - \frac{\left(\alpha_{1n}^2 \cosh \alpha_{1n} + \alpha_{2n}^2 \cos \alpha_{2n}\right)(\alpha_{2n} \sinh \alpha_{1n} - \alpha_{1n} \sin \alpha_{2n})}{\alpha_{1n}^2 \sinh \alpha_{1n} + \alpha_{1n}\alpha_{2n} \sin \alpha_{2n}}\right] A_n \tag{47}$$

If equations (46) and (47) are substituted into equations (44) and (45), the n^{th} mode shape for an array in a 1-g field can be determined to within an arbitrary factor A_n. For the 0-g field the boom equation given by equations (44) and (46) remains unchanged. The blanket equation for this case becomes

$$\bar{w}_n(\bar{x}) = D_n \sin \alpha_{3n}\bar{x} \tag{48}$$

In addition, for the 0-g field the boundary condition given by equation (28) yields the following result for D_n:

$$D_n = \frac{F_1(\bar{\beta}_n)}{\sin \alpha_{3n}} C_n \tag{49}$$

Thus, equations (44), (46), (48), and (49) determine the n^{th} mode for an array in a 0-g field. The mode shapes for the torsional cases can be developed in an analogous manner.

The orthogonality relations for the solar array can be developed in a straightforward manner. Because of the length of this development it is given in appendix C.

Summary of continuum mechanics approach. - In the previous sections the mode shapes and frequencies of a split-blanket solar array were determined by solving the

differential equations governing the motion of the system. The results showed that the array will exhibit symmetric or bending modes and antisymmetric or torsional modes of vibration. The frequencies of the bending modes can be found by solving equation (33) or (42) for an array in a 1-g or a 0-g field, respectively. Similarly, the torsional mode frequencies can be determined from equation (37), (38), or (43) depending on the particular case of interest. In all of these cases a highly transcendental equation involving Bessel functions and/or trigonometric and hyperbolic functions must be solved numerically to obtain a solution. In the following section an alternative approach is developed that uses the Rayleigh-Ritz method. This approach can readily be extended to include more complex arrays for which exact solutions cannot be found.

Rayleigh-Ritz Approach

In the Rayleigh-Ritz method (ref. 9) the strain energy and kinetic energy of the system are expressed in terms of (1) assumed modes that are functions of the spatial coordinates and (2) unknown generalized coordinates that are functions of time. By using Lagrange's equation and these energy expressions a set of second-order, linear, differential equations in terms of the generalized coordinates can be obtained. This set of equations is then reduced to an eigenvalue problem from which the modes and frequencies can be determined.

The success of the method is highly dependent on choosing a proper finite set of assumed modes that will ensure accurate results. The method, as applied to a large solar array, is now developed for the array bending vibrations and the results compared with the exact results of the previous section.

Strain energy of system in bending. - Let $N_x^{(0)}$ be the uniform stress resultant in the blanket when it is in its static equilibrium configuration. During the motion of the blanket about this equilibrium configuration the resultant stress will change to N_x. Assume that the stress induced by motion is small relative to $N_x^{(0)}$ so that $N_x \approx N_x^{(0)}$. Under these conditions it can be shown (ref. 11) that for small displacements the change in strain energy in the blanket U_m is given by

$$U_m = \frac{1}{2} \int_{-b/2}^{b/2} \int_0^{l} N_x^{(0)} \left(\frac{\partial W}{\partial x} \right)^2 dx\, dy \tag{50}$$

For an array hanging vertically in a 1-g field the resultant stress is given by equation (3) as

$$N_x^{(0)} = \frac{P}{b}\left(1 + \frac{1}{\bar{P}} - \frac{\bar{x}}{\bar{P}}\right) \tag{51}$$

From equations (50) and (51) the blanket strain energy in nondimensional form is

$$U_m = \frac{P\ell}{2}\int_0^1 \left(1 + \frac{1}{\bar{P}} - \frac{\bar{x}}{\bar{P}}\right)\left(\frac{\partial \bar{W}}{\partial \bar{x}}\right)^2 d\bar{x} \tag{52}$$

where $\bar{W} = W/\ell$. Similarly, it can be shown (ref. 12) that the strain energy in the boom U_b is given by

$$U_b = \frac{1}{2}\frac{EI}{\ell}\left[\int_0^1 \left(\frac{\partial^2 \bar{V}}{\partial \bar{x}^2}\right)^2 d\bar{x} - \bar{k}^2 \int_0^1 \left(\frac{\partial \bar{V}}{\partial \bar{x}}\right)^2 d\bar{x}\right] \tag{53}$$

where $\bar{V} = V/\ell$. The total strain energy in the array is then

$$U = U_m + U_b \tag{54}$$

Kinetic energy of system in bending. - The kinetic energy of the array consists of the kinetic energy of the boom, blanket, and tip piece. The kinetic energy of the blanket T_m is

$$T_m = \frac{1}{2}\int_0^\ell \rho_m \left(\frac{\partial W}{\partial t}\right)^2 dx = \frac{1}{2} M_m \ell^2 \int_0^1 \left(\frac{\partial \bar{W}}{\partial t}\right)^2 d\bar{x} \tag{55}$$

Similarly, the kinetic energy of the boom T_b is

$$T_b = \frac{M_b \ell^2}{2}\int_0^1 \left(\frac{\partial \bar{V}}{\partial t}\right)^2 d\bar{x} \tag{56}$$

Lastly, the kinetic energy of the tip piece T_{tp} is

$$T_{tp} = \frac{1}{2} M_{tp} \ell^2 \left[\frac{\partial V}{\partial t}(1,t)\right]^2 \tag{57}$$

The total kinetic energy of the array is then given by

$$T_T = T_m + T_b + T_{tp} \tag{58}$$

Energy expressions in terms of generalized coordinates. - To express the strain and kinetic energies in terms of generalized coordinates, the displacements $\overline{W}$ and $\overline{V}$ are assumed to be represented by the following series:

$$\overline{V}(\overline{x},t) = \sum_{1}^{N} q_n(t)\overline{\eta}_n(\overline{x}) \tag{59a}$$

$$\overline{W}(\overline{x},t) = \overline{x} \sum_{1}^{N} q_n(t)\overline{\eta}_n(1) + \sum_{1}^{M} q_{N+n}(t) \sin n\pi\overline{x} \tag{59b}$$

In equations (59), η_n represents a set of specified functions that are linearly independent over the range $0 \le \overline{x} \le 1$ and satisfy, at least, the geometric boundary conditions for the boom. Also, the time-dependent functions q_n represent the unknown generalized coordinates. Note that equations (59) satisfy the compatibility of displacement at the tip. Using the assumed solution given by equations (59) in the expression given for strain energy by equation (54) yields, after evaluating the resulting integrals, the following equation for strain energy:

$$U = \frac{EI}{2\ell}\left\{\sum_{1}^{N}\sum_{1}^{N} K_{mn} q_n q_m + \frac{2\overline{k}^2}{\pi\overline{P}} \sum_{n=1}^{N}\sum_{m=1}^{M}\left[\frac{1-(-1)^m}{m}\right]\overline{\eta}_n(1) q_n q_{N+m}\right.$$

$$\left. + \overline{k}^2 \sum_{1}^{M}\sum_{1}^{M} mn\left[\frac{\pi^2}{2}\left(1 + \frac{1}{2\overline{P}}\right)\delta_{mn} + b_{mn}\right] q_{N+n} q_{N+m}\right\} \tag{60}$$

where K_{mn}, b_{mn}, and δ_{mn} (Kronecker delta function) are defined as follows:

$$K_{mn} = \int_0^1 \bar{\eta}_n'' \bar{\eta}_m'' \, d\bar{x} - \bar{k}^2 \left[\int_0^1 \bar{\eta}_m' \bar{\eta}_n' \, d\bar{x} - \left(1 + \frac{1}{2\bar{P}}\right) \bar{\eta}_n(1) \bar{\eta}_m(1) \right] \tag{61}$$

$$b_{mn} = \begin{cases} 0 & \text{for } m = n \\ \left[1 - (-1)^{m+n}\right] \left[\dfrac{m^2 + n^2}{\left(m^2 - n^2\right)^2} \right] & \text{for } m \neq n \end{cases} \tag{62}$$

$$\delta_{mn} = \begin{cases} 0 & \text{for } m \neq n \\ 1 & \text{for } m = n \end{cases} \tag{63}$$

Similarly, from equations (59) and (58) the expression for kinetic energy becomes

$$T = \frac{1}{2} M_b \ell^2 \left[\sum_1^N \sum_1^N G_{mn} \dot{q}_n \dot{q}_m + \frac{2\bar{M}_m}{\pi} \sum_{n=1}^N \sum_{m=1}^M \frac{(-1)^{m+1}}{m} \dot{q}_n \dot{q}_{N+m} + \frac{\bar{M}_m}{2} \sum_1^M \dot{q}_{N+n}^2 \right] \tag{64}$$

where

$$G_{mn} = \int_0^1 \bar{\eta}_n \bar{\eta}_m \, d\bar{x} + \left(\frac{1}{3} \bar{M}_m + \bar{M}_{tp}\right) \bar{\eta}_n(1) \bar{\eta}_m(1) \tag{65}$$

Equations (60) and (64) represent the strain and kinetic energies in terms of $N + M$ generalized coordinates q_i. The equations of motion can now be written in terms of the generalized coordinates by a direct application of Lagrange's equation.

Equations of motion. - Lagrange's equation is given by

$$\frac{d}{dt}\left(\frac{\partial T}{\partial \dot{q}_r}\right) + \frac{\partial U}{\partial q_r} = 0 \qquad \text{for } r = 1, 2, \ldots, N, N+1, N+2, N+M \tag{66}$$

From equations (60) and (64), equation (66) yields for $1 \leq r \leq N$ the following set of equations:

$$\frac{M_b \ell^3}{EI}\left[\sum_1^N G_{rn}\ddot{q}_n + \frac{2\overline{M}_m}{\pi}\bar{\eta}_r(1)\sum_1^M \frac{(-1)^{m+1}}{m}\ddot{q}_{N+m}\right]$$

$$+\left\{\sum_1^N K_{nr}q_n + \frac{\bar{k}^2\bar{\eta}_r(1)}{\pi\overline{\overline{P}}}\sum_1^M\left[\frac{1-(-1)^m}{m}\right]q_{N+m}\right\} = 0 \qquad \text{for } r = 1,2,\ldots,N \tag{67}$$

Similarly, for $N + 1 \leq r \leq N + M$ these equations yield

$$\frac{M_b \ell^3}{EI}\left[\frac{\overline{M}_m}{\pi}\frac{(-1)^{r+1}}{r}\sum_1^N \bar{\eta}_n(1)\ddot{q}_n + \frac{\overline{M}_m}{2}\ddot{q}_{N+r}\right] + \left\{\frac{\bar{k}^2}{\pi\overline{\overline{P}}}\left[\frac{1-(-1)^r}{r}\right]\sum_1^N \bar{\eta}_n(1)q_n\right.$$

$$\left.+\bar{k}^2\sum_1^M rn\left[\frac{\pi^2}{2}\left(1+\frac{1}{2\overline{\overline{P}}}\right)\delta_{rn} + \frac{b_{rn}}{\overline{\overline{P}}}\right]q_{N+n}\right\} = 0 \qquad \text{for } r = 1,2,\ldots,M \tag{68}$$

Equations (67) and (68) represent the equations of motion in terms of generalized coordinates. In matrix notation these equations can be expressed as

$$\frac{M_b \ell^3}{EI}[\overline{M}]\{\ddot{q}\} + [\overline{K}]\{q\} = \{0\} \tag{69}$$

where $[\overline{M}]$ and $[\overline{K}]$ are $(N + M) \times (N + M)$ symmetric, nondimensional mass and stiffness matrices, respectively, and $\{q\}$ is a $(N + M) \times 1$ vector of the generalized coordinates. Equation (69) can be expressed in partitioned form as

$$\frac{M_b \ell^2}{EI}\left[\begin{array}{c|c} \overline{M}^{11} & \overline{M}^{12} \\ (N \times N) & (N \times M) \\ \hline \overline{M}^{21} & \overline{M}^{22} \\ (M \times N) & (M \times M) \end{array}\right]\left\{\begin{array}{c} \ddot{q}_1 \\ \ddot{q}_2 \\ \cdot \\ \cdot \\ \ddot{q}_N \\ \hline \ddot{q}_{N+1} \\ \cdot \\ \cdot \\ \ddot{q}_{M+N} \end{array}\right\} + \left[\begin{array}{c|c} \overline{K}^{11} & \overline{K}^{12} \\ (N \times N) & (N \times M) \\ \hline \overline{K}^{21} & \overline{K}^{22} \\ (M \times N) & (M \times M) \end{array}\right]\left\{\begin{array}{c} q_1 \\ q_2 \\ \cdot \\ \cdot \\ q_N \\ \hline q_{N+1} \\ \cdot \\ \cdot \\ q_{M+N} \end{array}\right\} = \left\{\begin{array}{c} 0 \\ 0 \\ \cdot \\ \cdot \\ 0 \\ \hline 0 \\ \cdot \\ \cdot \\ 0 \end{array}\right\} \tag{70}$$

where the elements of the submatrices $[M^{mn}]$ and $[\overline{K}^{mn}]$, m, n = 1, 2 are given, using equations (67) and (68), by the following:

$$\overline{M}_{ij}^{11} = G_{ij} \qquad \text{for } i,j = 1,2,\ldots,N \tag{71a}$$

$$\overline{M}_{ij}^{22} = \frac{\overline{M}_m}{2}\delta_{ij} \qquad \text{for } i,j = 1,2,\ldots,M \tag{71b}$$

$$\overline{M}_{ij}^{12} = \overline{M}_{ji}^{21} = \frac{\overline{M}_m}{\pi}\overline{\eta}_i(1)\frac{(-1)^{j+1}}{j} \qquad \text{for } i = 1,2,\ldots,N;\ j = 1,2,\ldots,M \tag{71c}$$

$$\overline{K}_{ij}^{11} = K_{ij} \qquad \text{for } i,j = 1,2,\ldots,N \tag{71d}$$

$$\overline{K}_{ij}^{22} = \frac{\pi^2\overline{k}^2}{2}\left(1 + \frac{1}{2\overline{P}}\right)i^2\delta_{ij} + \frac{\overline{k}^2}{P}b_{ij} \qquad \text{for } i,j = 1,2,\ldots,M \tag{71e}$$

$$\overline{K}_{ij}^{12} = \overline{K}_{ji}^{21} = \frac{2\overline{k}^2}{\pi\overline{P}}\left\{\overline{\eta}_i(1)\left[\frac{1-(-1)^j}{2j}\right]\right\} \qquad \text{for } i = 1,2,\ldots,N;\ j = 1,2,\ldots,M \tag{71f}$$

When the set of N assumed modes of the boom $\overline{\eta}_n(x)$ are specified, equation (71) can be used to generate the mass and stiffness matrices for any value of M. Equation (69) represents a set of linear, second-order differential equations whose solution is given by

$$\{\ddot{q}\} = -\omega^2\{q\} \tag{72}$$

where ω is the angular natural frequency of the system. Substituting equation (72) into equation (69) and multiplying through by $[K]^{-1}$ yield

$$[\bar{K}]^{-1}[\bar{M}]\{q\} = \frac{1}{\bar{\beta}^4}\{q\} \tag{73}$$

Equation (73) represents an eigenvalue problem whose solution is discussed in numerous texts on vibration theory (see e.g., ref. 9 or ref. 13).

Mass and stiffness matrices using cantilevered beam mode shapes. - As previously stated, the success of equation (73) in predicting the mode shapes and frequencies of the array depends primarily on the choice of assumed modes $\bar{\eta}_n(x)$. An obviously good choice for this generating set that satisfies all the required geometric boundary conditions would be the modal functions of a uniform cantilevered beam. In this section the mass and stiffness matrices given by equation (70) will be developed based on these assumed modes. The mode shapes for a uniform cantilevered beam are given by reference 14

$$\bar{\eta}_n(\bar{x}) = \cosh(\bar{\beta}_{cn}\bar{x}) - \cos(\bar{\beta}_{cn}\bar{x}) - \alpha_{cn}\left[\sinh(\bar{\beta}_{cn}\bar{x}) - \sin(\bar{\beta}_{cn}\bar{x})\right] \tag{74}$$

where $\bar{\beta}_{cn}$ is the frequency parameter for a cantilevered beam and α_{cn} is a function of $\bar{\beta}_{cn}$. If ω_{cn} is the n^{th} angular natural frequency of the beam,

$$\left.\begin{aligned} \bar{\beta}_{cn}^4 &= \frac{M_b \ell^3}{EI}\omega_{cn}^2 \\ \alpha_{cn} &= \frac{\sinh \bar{\beta}_{cn} - \sin \bar{\beta}_{cn}}{\cosh \bar{\beta}_{cn} + \cos \bar{\beta}_{cn}} \end{aligned}\right\} \tag{75}$$

Values for $\bar{\beta}_{cn}$ and α_{cn} as given in reference 14 are included in this report in table I. From equation (74) and the well-known orthogonality conditions for uniform beams, the following relations exist:

$$\left.\begin{aligned} \int_0^1 \bar{\eta}_n \bar{\eta}_m \, d\bar{x} &= \delta_{mn} \\ \int_0^1 \bar{\eta}_n'' \bar{\eta}_m'' \, d\bar{x} &= \delta_{mn}\bar{\beta}_{cn}^4 \end{aligned}\right\} \tag{76}$$

It can also be shown after a considerable amount of manipulation that the following relations are valid for the assumed mode shape:

$$\left.\begin{aligned} \bar{\eta}_n(1) &= 2(-1)^{n+1} \\ \int_0^1 \bar{\eta}_n'^2 \, d\bar{x} &= \alpha_{cn}\bar{\beta}_{cn}(2 + \alpha_{cn}\bar{\beta}_{cn}) \\ \int_0^1 \bar{\eta}_n'\bar{\eta}_m' \, d\bar{x} &= \frac{4(-1)^{n+m}\bar{\beta}_{cn}\bar{\beta}_{cm}}{\bar{\beta}_{cn}^2 - (-1)^{n+m}\bar{\beta}_{cm}^2}\left[\bar{\beta}_{cn}\alpha_{cm} - (-1)^{n+m}\bar{\beta}_{cm}\alpha_{cn}\right] \end{aligned}\right\} \quad (77)$$

From equations (61), (65), (71), (76), and (77) the elements of the mass and stiffness submatrices are given by the following:

$$\bar{M}_{ij}^{11} = \delta_{ij} + 4\left(\frac{1}{3}\bar{M}_m + \bar{M}_{tp}\right)(-1)^{i+j} \quad (78a)$$

$$\bar{M}_{ij}^{12} = \bar{M}_{ji}^{21} = \frac{2\bar{M}_m}{\pi}\frac{(-1)^{i+j}}{j} \quad (78b)$$

$$\bar{K}_{ii}^{11} = \bar{\beta}_{ci} - \bar{k}^2\left[\bar{\beta}_{ci}\alpha_{ci}(2 + \bar{\beta}_{ci}\alpha_{ci}) - 4\left(1 + \frac{1}{2\bar{P}}\right)\right] \quad (78c)$$

$$\bar{K}_{ij}^{11} = -\bar{k}^2\left\{\frac{4(-1)^{i+j}\bar{\beta}_{ci}\bar{\beta}_{cj}}{\bar{\beta}_{ci}^2 - (-1)^{i+j}\bar{\beta}_{cj}}\left[\bar{\beta}_{ci}\alpha_{cj} - (-1)^{i+j}\bar{\beta}_{cj}\alpha_{ci}\right] - 4(-1)^{i+j}\left(1 + \frac{1}{2\bar{P}}\right)\right\} \quad (i \neq j) \quad (78d)$$

$$\bar{K}_{ij}^{12} = \bar{K}_{ji}^{21} = \frac{2\bar{k}^2}{\pi\bar{P}}\left\{\frac{(-1)^{i+1}}{j}\left[1 - (-1)^j\right]\right\} \quad (78e)$$

From equations (78), (71b), and (71e) the mass and stiffness matrices can be determined when the mass ratios $\bar{M}_m$ and $\bar{M}_{tp}$ and the load parameters $\bar{k}$ and $\bar{P}$ are specified. Note that these matrices are valid for both the 1-g and 0-g configurations. For the 0-g case, $1/\bar{P}$ is set equal to zero in equations (78c), (78d), and (78e).

Two-mode approximation using preloaded cantilevered beam mode. - For the 0-g

configuration a good approximation for the first two lowest bending frequencies can be obtained by using an assumed mode corresponding to the first mode of a uniform cantilevered beam under directed axial load (ref. 8). It can be expected that this type of assumed mode will give more accurate results than the results of the previous section for a two-mode approximation, since it more nearly approximates the condition of the boom in the array. Now for $N = 1$ and $M = 1$ the solution to equation (70) becomes

$$\left.\begin{aligned}\left(K_{11} - \bar{\beta}^4 G_{11}\right)q_1 - \bar{\beta}^4 \frac{\bar{M}_m}{\pi}\bar{\eta}_1(1)q_2 = 0 \\ -\bar{\beta}^4 \frac{\bar{M}_m}{\pi}\bar{\eta}_1(1)q_1 + \frac{1}{2}\left(\pi^2\bar{k}^2 - \bar{\beta}^4\bar{M}_m\right)q_2 = 0\end{aligned}\right\} \tag{79}$$

Equating the determinant of the coefficients of the unknowns in equations (79) to zero yields the characteristic equation given by

$$A_2\bar{\beta}^8 - B_2\bar{\beta}^4 + C_2 = 0 \tag{80}$$

where

$$A_2 = G_{11}\bar{M}_m - 2\left[\frac{\bar{M}_m}{\pi}\bar{\eta}_1(1)\right] \tag{81a}$$

$$B_2 = \pi^2\bar{k}^2 G_{11} + M_m K_{11} \tag{81b}$$

$$C_2 = \pi^2 K_{11}\bar{k}^2 \tag{81c}$$

Equation (80) is a quadratic equation in $\bar{\beta}^4$ that can be solved once the coefficients A_2, B_2, and C_2 are known. These coefficients, which are given by equations (81), can be written in terms of the beam mode by using equations (61) and (65) for G_{11} and K_{11}. From equation (65)

$$G_{11} = \int_0^1 \bar{\eta}_1^2 \, d\bar{x} + \left(\frac{1}{3}\bar{M}_m + \bar{M}_{tp}\right) \tag{82}$$

Next from equation (61) and the orthogonality relations for a cantilevered beam under directed axial load,

$$K_{11} = \bar{\beta}_{d1}^4 \int_0^1 \bar{\eta}_1^2 \, d\bar{x} \tag{83}$$

where $\bar{\beta}_{d1}$ is the frequency parameter. Substituting equations (82) and (83) into equations (81) and noting that $\bar{k} = \pi^2 P/P_{cr,0}$ yield

$$A_2 = \bar{M}_m \left\{ \int_0^1 \bar{\eta}_1^2 \, d\bar{x} + \left[\bar{M}_m \left(\frac{1}{3} - \frac{2}{\pi^2} \right) + \bar{M}_{tp} \right] \bar{\eta}_1^2(1) \right\} \tag{84a}$$

$$B_2 = \left[\left(\pi^4 \frac{P}{P_{cr,0}} + \bar{M}_m \bar{\beta}_{d1}^4 \right) \int_0^1 \bar{\eta}_1^2 \, d\bar{x} + \pi^4 \frac{P}{P_{cr,0}} \left(\frac{1}{3} \bar{M}_m + \bar{M}_{tp} \right) \bar{\eta}_1^2(1) \right] \tag{84b}$$

$$C_2 = \pi^4 \frac{P}{P_{cr,0}} \bar{\beta}_{d1}^4 \int_0^1 \bar{\eta}_1^2 \, d\bar{x} \tag{84c}$$

Equations (84) describe the coefficients in equation (80) in terms of the parameters β_{d1}, $\bar{\eta}_1(1)$, and $\int_0^1 \bar{\eta}_1^2 \, d\bar{x}$ for a cantilevered beam under directed axial load. As shown in reference 8 these parameters are a function of $\bar{k}$ or $P/P_{cr,0}$. Table II, which was developed from the results of reference 8, gives the values for these parameters as a function of $P/P_{cr,0}$. Thus, from this table the coefficients A_2, B_2, and C_2 can be determined for the various values of $P/P_{cr,0}$, and the first and second lowest frequencies can subsequently be determined from equation (80).

RESULTS AND DISCUSSION

Continuum Mechanics Approach

To determine the effect of the various parameters on the frequencies of a split-blanket solar array in both a 0-g and a 1-g cantilevered configuration, equations (33), (38), (42), and (43) were solved numerically by the method of bisection (ref. 15). The results for the first three bending frequencies for the 0-g case are shown in figures 5, 6, and 7. These figures show the variation in frequencies as a function of the axial load ratio $P/P_{cr,0}$ and the mass parameters $\bar{M}_{tp}$ and $\bar{M}_m$. The tip-piece mass parameter $\bar{M}_{tp}$ was varied between 0 and 40 and the blanket mass parameter $\bar{M}_m$ was varied between 1 and 6. This should cover the useful range of these parameters. The axial

load ratio $P/P_{cr,0}$ represents the ratio of boom load to buckling load of the array in a 0-g configuration; that is, $P_{cr,0} = \pi^2 EI/l^2$. Thus, when $P/P_{cr,0} = 0$ (blanket tension of zero) and when $P/P_{cr,0} = 1$, the frequency parameter $\overline{\beta}_1$ is zero. It follows then that at some point between 0 and 1, $\overline{\beta}_1$ reaches a maximum. This implies that for a given array ($\overline{M}_m$ and $\overline{M}_{tp}$ fixed) there is an optimum preload P that will yield a maximum fundamental frequency. This, of course, may not correspond to the minimum frequency of the array since the fundamental torsional frequency must also be considered. However, it does appear that this optimum preload may be significant in designing a lightweight solar array.

Similarly, figures 8 and 9 illustrate the variation in the fundamental and second bending frequencies of a solar array suspended vertically in a 1-g field. In addition to the parameters used for the 0-g case, an additional parameter must be specified for the 1-g configuration, namely, $P_{cr,0}/W_m$. For the graphs shown in these figures, $P_{cr,0}/W_m = 1$. Note from figure 8 that when $P/P_{cr,0} \approx 1.52$, $\overline{\beta}_1 = 0$. This implies that the buckling load of the array is given by $P_{cr} \approx 1.52\ P_{cr,0}$. This result has been checked by solving the buckling equation for the array given in appendix A by equation (A14). This equation has also been solved for various values of $W_m/P_{cr,0}$, and the results are presented in figure 10. This figure gives the buckling load of an array suspended vertically in a 1-g field as a function of blanket weight.

Figures 11 and 12 show the effects of both tip-piece mass inertia and torsional beam stiffness on the fundamental and second torsional frequencies of an array in a 0-g and a 1-g configuration, respectively. As in the bending case, the torsional frequencies of an array in a 1-g field are illustrated by taking $P_{cr,0}/W_m = 1$.

Finally, figure 13 illustrates the effect of axial load on the mode shapes of a solar array in a 0-g field. The mode shapes were determined from equations (44) and (48) for values of $\overline{M}_n = 3$ and $\overline{M}_{tp} = 1$. These figures show that the mode shapes can be very dependent on the axial load. For small loads (figs. 13(a) to (c)), the first three modes are predominately blanket modes. For the point where the fundamental bending frequency is a maximum (figs. 13(d) to (f)), both blanket and boom participate equally in the modal displacement. For larger loads (figs. 13(g) to (i)), the first mode is predominately a beam mode, but the second and third modes show a coupling effect.

Rayleigh-Ritz Approach

The Rayleigh-Ritz method presents an alternate and somewhat simpler approach for determining the modes and frequencies of a split-blanket solar array. The accuracy of this method depends primarily on the type and number of assumed functions used to generate the required mass and stiffness matrices given in equation (70). The accuracy of this method, which uses cantilevered beam modes for the boom and string modes for the

blanket, was investigated by solving the eigenvalue problem given in equation (73). This equation was solved for various mass ratios $\overline{M}_{tp}$ and $\overline{M}_{m}$ and axial load ratios $P/P_{cr,0}$. Both 0-g and 1-g configurations were investigated.

The eigenvalue problem was solved by matrix iteration to find the lowest, or dominant, frequency parameter of the system. The higher modes and frequencies were determined by the technique known as "deflation" of a matrix. This method uses the orthogonality conditions that exist between the modes to sweep out the known, lower modes from the dynamic matrix given by $K^{-1}M$. This technique is well described in references 9 and 13.

Typical results and comparisons with exact results for the 0-g and 1-g configurations are shown in tables III and IV. These tables indicate that good results, at least for the first three frequencies, can be obtained in most cases by taking three beam modes for the boom and three string modes for the blanket. These tables also illustrate the improvement in accuracy achieved by increasing the number of assumed modes.

In addition to the solutions for equation (73), table III also gives the solution to equation (80). This equation is based on a two-mode approximation that uses the first mode of a cantilevered beam under a directed axial load and the first string mode. Parameters required in the solution of equation (80) relating to the modal characteristics of a beam under directed axial loads were developed from the equations presented in reference 8 and are given in table III. The exact results are compared with the two-mode approximate results in table III and there is good agreement, for the fundamental frequency, for all values of $P/P_{cr,0}$. Also, for the second frequency the error is less than 1 percent, provided that $P/P_{cr,0} > 0.08$.

CONCLUDING REMARKS

Two methods have been presented for calculating the modes and frequencies of a large split-blanket solar array in both a 0-g and a 1-g cantilevered configuration. The first method is based on the equations of continuum mechanics; the second method is based on the Rayleigh-Ritz, or assumed mode, approach.

The continuum mechanics approach results in a highly transcendental equation that must be solved by numerical techniques. This has been done for a wide range of solar array parameters, and the results have been presented in graphical form.

The Rayleigh-Ritz approach uses cantilevered beam modes to represent the boom displacement and string modes to represent the blanket displacement. Based on these assumed modes the mass and stiffness matrices of the array were developed for an arbitrary number of assumed modes. The resulting eigenvalue problem was then solved by matrix iteration for an increasing number of assumed modes. The results were then compared with the exact results of the first method. This comparison disclosed that

good results are obtained for the lower bending frequencies by using a relatively small number of assumed modes.

Lastly, a two-mode approximation for an array in a 0-g configuration was presented. The assumed modes used for this case consisted of the first cantilevered mode for a uniform beam under directed axial load and the first string modes. The characteristic equation for this case is a quadratic equation that can be solved in closed form for the first and second bending frequencies. These results compared well with the exact solution for all the cases investigated. This type of solution can be used to determine the first two lowest bending frequencies of a solar array very rapidly without the aid of a computer.

Lewis Research Center,
National Aeronautics and Space Administration,
Cleveland, Ohio, July 22, 1976,
506-22.

APPENDIX A

BUCKLING LOAD FOR A SOLAR ARRAY IN A 1-g FIELD

The buckling load for a solar array in a 1-g field can be determined from the equations of motion with the acceleration terms set equal to zero. From equations (2), (6b), (7), and (11) these equations in nondimensional form are

$$\frac{d}{d\bar{x}}\left(\bar{T}\frac{d\bar{w}}{d\bar{x}}\right) = 0 \tag{A1}$$

$$\frac{d^4\bar{v}}{d\bar{x}^4} + \bar{k}^2\frac{d^2\bar{v}}{d\bar{x}^2} = 0 \tag{A2}$$

$$\frac{d^3\bar{v}(1)}{d\bar{x}^3} + \bar{k}^2\frac{d\bar{v}(1)}{d\bar{x}} - \bar{k}^2\frac{d\bar{w}(1)}{d\bar{x}} = 0 \tag{A3}$$

where $\bar{k} = P\ell^2/EI$ and $\bar{T}$ is the nondimensional blanket tension given by equation (4) as

$$\bar{T} = \frac{T_b}{P} = 1 + \frac{1}{\bar{P}} - \frac{\bar{x}}{\bar{P}} \tag{A4}$$

The boundary conditions and compatibility relation for this case are

$$\bar{w}(0) = 0 \tag{A5}$$

$$\left.\begin{aligned} \bar{v}(0) &= 0 \\ \frac{d\bar{v}(0)}{d\bar{x}} &= 0 \\ \frac{d^2\bar{v}(1)}{d\bar{x}^2} &= 0 \end{aligned}\right\} \tag{A6}$$

$$\bar{w}(1) = \bar{v}(1) \tag{A7}$$

The buckling load can be determined by solving equations (A1) and (A2) subject to condi-

tions (A3) and (A5) to (A7). Thus, from equations (A1) and (A4)

$$\frac{d\overline{w}}{d\overline{x}} = \frac{C}{1 + \frac{1}{\overline{P}} - \frac{\overline{x}}{\overline{P}}} \tag{A8}$$

Integrating this equation and applying the boundary condition given by equation (A5)

$$\overline{w}(x) = C\overline{P} \ln\left(\frac{1 + \overline{P}}{1 + \overline{P} - \overline{x}}\right) \tag{A9}$$

Next the solution to equation (A2) is

$$\overline{v}(\overline{x}) = A \sin \overline{kx} + \overline{B} \cos \overline{kx} + D\overline{x} + E \tag{A10}$$

Using the boundary conditions given by equations (A6) gives the following relations:

$$\left.\begin{aligned} A &= -\frac{D}{\overline{k}} \\ B &= \frac{D}{\overline{k}} \tan \overline{k} \\ E &= -\frac{D}{\overline{k}} \tan \overline{k} \end{aligned}\right\} \tag{A11}$$

Substituting equations (A11) into (A10) yields

$$\overline{v}(\overline{x}) = \frac{D}{\overline{k}} [\tan \overline{k}(\cos \overline{k} - 1) - \sin \overline{kx} + \overline{kx}] \tag{A12}$$

Equations (A9) and (A12) now contain two unknowns, C and D, which can be evaluated by using the two remaining conditions given by equations (A3) and (A7). The condition given by equation (A3) yields

$$C = D \tag{A13}$$

and using (A13) in addition to (A9) and (A12) in equation (A7) yields

$$\tan \bar{k} = \bar{k}\left[1 - \bar{P} \ln\left(1 + \frac{1}{\bar{P}}\right)\right] \tag{A14}$$

Equation (A14) is the characteristic equation from which the critical buckling load P_{cr} can be determined. Note that when $\bar{P} \to \infty$ (i.e., $W_m \to 0$) the right side of equation (A14) becomes zero and the solution to (A14) yields

$$P_{cr,0} = \frac{\pi^2 EI}{\ell^2} \tag{A15}$$

which is the critical buckling load of the array in a 0-g field. Expression $\bar{k}$ and $\bar{P}$ in terms of $P_{cr,0}$ gives the following relations:

$$\bar{P} = \frac{P}{W_m} = \left(\frac{P}{P_{cr,0}}\right)\left(\frac{P_{cr,0}}{W_m}\right)$$

$$\bar{k} = \frac{P\ell^2}{EI} = \left(\frac{P}{P_{cr,0}}\right)\left(\frac{P_{cr,0}\ell^2}{EI}\right) = \pi^2 \frac{P}{P_{cr,0}} \tag{A16}$$

By using (A16) in (A14), $P_{cr}/P_{cr,0}$ can be determined as a function of $W_m/P_{cr,0}$.

APPENDIX B

ASYMPTOTIC FORMULAS FOR $F_1(\bar{\beta})$, $F_2(\bar{\beta})$, $F_3(\bar{\beta}_t)$, AND $F_4(\bar{\beta}_t)$

The characteristic equations for bending and torsion of a solar array in a 1-g field contain certain functions that can be evaluated more simply for large values of their arguments. This will be the case when the blanket weight W_m approaches zero. To simplify the writing of these equations, let

$$z_1 = \kappa_1 \bar{\beta}^2 \tag{B1}$$

where

$$\kappa_1 = \frac{\bar{M}_m^{1/2} \bar{P}}{\bar{k}} \tag{B2}$$

In terms of z_1, equations (30) and (32) become

$$F_1(\bar{\beta}) = J_0(2z_1)Y_0(2z_1\zeta_0) - Y_0(2z_1)J_0(2z_1\zeta_0) \tag{B3}$$

$$F_2(\bar{\beta}) = \frac{1}{J_0(2z_1)}\left[z_1 J_1(2z_1)F_1(\bar{\beta}) + \frac{1}{\pi} J_0(2z_1\zeta_0)\right] \tag{B4}$$

Now, as W_m approaches 0, z_1 approaches ∞ and the arguments of the Bessel functions in equations (B3) and (B4) become large. Thus, the asymptotic formulas for these functions can be used. For large values of z_1 these formulas as given by reference 10 are

$$\left.\begin{aligned} J_0(2z_1) &= \sqrt{\frac{1}{\pi z_1}} \cos\left(2z_1 - \frac{\pi}{4}\right) \\ Y_0(2z_1) = J_1(2z_1) &= \sqrt{\frac{1}{\pi z_1}} \sin\left(2z_1 - \frac{\pi}{4}\right) \end{aligned}\right\} \tag{B5}$$

Similar expressions exist for $J_0(2z_1\zeta_0)$ and $Y(2z_1\zeta_0)$. From equations (B5) and (B3), $F_1(\bar{\beta})$ reduces to

$$F_1(\bar{\beta}) = \frac{1}{\pi z_1 \zeta_0^{1/2}} \sin[2z_1(\zeta_0 - 1)] \tag{B6}$$

Now for small values of W_m or large values of $\bar{P}$, equation (B2) yields for the term in brackets in equation (B6)

$$2z_1(\zeta_0 - 1) = 2\kappa_1 \bar{\beta}^2(\zeta_0 - 1)$$

$$= \frac{2\bar{M}_m^{1/2}}{\bar{k}} \bar{\beta}^2 \bar{P} \left[\left(1 + \frac{1}{\bar{P}}\right)^2 - 1\right] \approx \alpha_3 \tag{B7}$$

where

$$\alpha_3 = \frac{\bar{M}_m^{1/2} \bar{\beta}^2}{\bar{k}} \tag{B8}$$

From equations (B6) and (B7)

$$F_1(\bar{\beta}) = \frac{1}{\pi \kappa_1 \bar{\beta}^2 \zeta_0^{1/2}} \sin \alpha_3 \tag{B9}$$

Next consider equation (B4) for large values of z_1. From equations (B5) this equation becomes, after a little manipulation,

$$F_2(\bar{\beta}) = \frac{1}{\pi \zeta_0} \cos[2z_1(\zeta_0 - 1)] \tag{B10}$$

The terms in brackets is again given by equation (B7). Noting that $\kappa_1 \bar{\beta}^2 = \alpha_3 \bar{P}$ (from eqs. (B2) and (B8)), equation (B10) can be written as

$$F_2(\bar{\beta}) = \frac{\alpha_3 \bar{P}}{\pi \zeta_0^{1/2} \kappa_1 \bar{\beta}^2} \cos \alpha_3 \tag{B11}$$

In a similar straightforward manner it can also be shown that $F_3(\bar{\beta}_t)$ and $F_4(\bar{\beta}_t)$ as given by equations (36) become for large values of $\bar{P}$

$$\left.\begin{aligned} F_3(\bar{\beta}_t) &= \frac{1}{\pi\kappa_2\zeta_0^{1/2}} \sin \bar{\beta}_t \\ F_4(\bar{\beta}_t) &= \frac{1}{\pi\zeta_0} \cos \bar{\beta}_t \end{aligned}\right\} \qquad \text{(B12)}$$

APPENDIX C

ORTHOGONALITY CONDITIONS

The orthogonality relations for the bending modes of a solar array in a 1-g field can be developed by starting with equations (18) and (19) and the corresponding boundary conditions given by equations (20) and (21). For an array vibrating in its i^{th} mode these equations become

$$\frac{d}{d\bar{\zeta}}\left(\bar{\zeta}\,\frac{d\bar{w}_i}{d\bar{\zeta}}\right) + 4\kappa_1^2\bar{\beta}_i^4(\bar{\zeta}\bar{w}_i) = 0 \tag{C1}$$

$$\frac{d^4\bar{v}_i}{d\bar{x}^4} + \bar{k}^2\,\frac{d^2\bar{v}_i}{d\bar{x}^2} - \bar{\beta}_i^4\bar{v}_i = 0 \tag{C2}$$

$$\frac{d^3\bar{v}_i(1)}{d\bar{x}^3} + \bar{k}^2\,\frac{d\bar{v}_i(1)}{d\bar{x}} + \frac{1}{2}\,\frac{\bar{k}^2}{\bar{P}}\,\frac{d\bar{w}_i(1)}{d\bar{\zeta}} + \bar{M}_{tp}\bar{\beta}_i^4\bar{v}_i(1) = 0 \tag{C3}$$

with boundary and compatibility conditions

$$\bar{v}_i(0) = 0 \tag{C4a}$$

$$\frac{d\bar{v}_i(0)}{d\bar{x}} = 0 \tag{C4b}$$

$$\bar{w}_i(\bar{\zeta}_0) = 0 \tag{C4c}$$

$$\bar{w}_i(1) = \bar{v}_i(1) \tag{C4d}$$

$$\frac{d^2\bar{v}_i(1)}{d\bar{x}^2} = 0 \tag{C4e}$$

First operate on equation (C1) by multiplying it by $\bar{w}_j$, where j corresponds to the j^{th} mode of vibration, and integrate over the length. This yields, after an integration by parts and applying conditions given by (C4c) and (C4d),

$$\bar{v}_j(1)\frac{d\bar{w}_i(1)}{d\zeta} - \int_{\zeta_0}^{1} \zeta \frac{d\bar{w}_i}{d\zeta}\frac{d\bar{w}_j}{d\zeta}\,d\bar{x} + 4\kappa_1^2\beta_i^4 \int_{\zeta_0}^{1} \zeta \bar{w}_i \bar{w}_j\,d\bar{x} = 0 \qquad \text{(C5)}$$

Next, multiply equation (C2) by $\bar{v}_j$ and integrate over the length to obtain

$$\int_0^1 \bar{v}_j \frac{d^4\bar{v}_i}{d\bar{x}^4}\,d\bar{x} + \bar{k}^2 \int_0^1 \bar{v}_j \frac{d^2\bar{v}_i}{d\bar{x}^2}\,d\bar{x} - \bar{\beta}_i^4 \int_0^1 \bar{v}_i \bar{v}_j\,d\bar{x} = 0$$

Integrating the first two integrals by parts and applying the boundary conditions given by equations (C4a) to (C4c) yield

$$\bar{v}_j(1)\left[\frac{d^3\bar{v}_i(1)}{d\bar{x}^3} + \bar{k}^2\frac{d\bar{v}(1)}{d\bar{x}}\right] + \int_0^1 \frac{d^2\bar{v}_i}{d\bar{x}^2}\frac{d^2\bar{v}_j}{d\bar{x}^2}\,d\bar{x} - \bar{k}^2 \int_0^1 \frac{d\bar{v}_i}{d\bar{x}}\frac{d\bar{v}_j}{d\bar{x}}\,d\bar{x}$$

$$- \bar{\beta}_i^4 \int_0^1 \bar{v}_i \bar{v}_j\,d\bar{x} = 0 \qquad \text{(C6)}$$

Subtracting equation (C3) from (C6) yields

$$-\frac{1}{2}\frac{\bar{k}^2}{\bar{P}}\bar{v}_j(1)\frac{d\bar{w}_i(1)}{d\zeta} + \int_0^1 \frac{d^2\bar{v}_i}{d\bar{x}}\frac{d\bar{v}_j}{d\bar{x}}\,d\bar{x} - \bar{k}^2 \int_0^1 \frac{d\bar{v}_i}{d\bar{x}}\frac{d\bar{v}_j}{d\bar{x}}\,d\bar{x}$$

$$- \bar{\beta}_i^4\left[\int_0^1 \bar{v}_i \bar{v}_j\,d\bar{x} + \bar{M}_{tp}\bar{v}_i(1)\bar{v}_j(1)\right] = 0 \qquad \text{(C7)}$$

The final step is to multiply equation (C5) by $\bar{k}^2/2\bar{P}$ and then add the resulting equation to equation (C7). The result, after noting that $\bar{k}^2\kappa_1^2/\bar{P} = \bar{M}_m\bar{P}$, is

$$\frac{\bar{k}^2}{2\bar{P}} \int_1^{\zeta_0} \zeta \frac{d\bar{w}_i}{d\zeta} \frac{d\bar{w}_j}{d\zeta} d\zeta + \int_0^1 \frac{d^2\bar{v}_i}{d\bar{x}^2} \frac{d^2\bar{v}_j}{d\bar{x}^2} d\bar{x} - \bar{k}^2 \int_0^1 \frac{d\bar{v}_i}{d\bar{x}} \frac{d\bar{v}_j}{d\bar{x}} d\bar{x}$$

$$- \bar{\beta}_i^4 \left[\int_0^1 \bar{v}_i \bar{v}_j \, d\bar{x} + 2\bar{M}_m \bar{P} \int_1^{\zeta_0} \zeta \bar{w}_i \bar{w}_j \, d\zeta + \bar{M}_{tp} \bar{v}_i(1) \bar{v}_j(1) \right] = 0 \qquad \text{(C8)}$$

If i and j are interchanged in equation (C8), a second equation is obtained that is similar to (C8) except that $\bar{\beta}_i^4$ is replaced by $\bar{\beta}_j^4$. Thus,

$$\frac{\bar{k}^2}{2\bar{P}} \int_0^{\zeta_0} \zeta \frac{d\bar{w}_i}{d\zeta} \frac{d\bar{w}_j}{d\zeta} d\zeta + \int_0^1 \frac{d^2\bar{v}_i}{d\bar{x}^2} \frac{d^2\bar{v}_j}{d\bar{x}^2} d\bar{x} - \bar{k}^2 \int_0^1 \frac{d\bar{v}_i}{d\bar{x}} \frac{d\bar{v}_j}{d\bar{x}} d\bar{x}$$

$$- \bar{\beta}_j^4 \left[\int_0^1 \bar{v}_i \bar{v}_j \, d\bar{x} + 2\bar{M}_m \bar{P} \int_1^{\zeta_0} \zeta \bar{w}_i \bar{w}_j \, d\zeta + \bar{M}_{tp} \bar{v}_i(1) \bar{v}_j(1) \right] = 0 \qquad \text{(C9)}$$

Subtracting equation (C9) from (C8) and defining the generalized mass as

$$M_i = \int_0^1 \bar{v}_i^2 \, d\bar{x} + 2\bar{M}_m P \int_1^{\zeta_0} \zeta \bar{w}_i \, d\zeta + \bar{M}_{tp} \bar{v}_i^2(1) \qquad \text{(C10)}$$

yields

$$\int_0^1 \bar{v}_i \bar{v}_j \, d\bar{x} + 2M_m \bar{P} \int_1^{\zeta_0} \zeta \bar{w}_i \bar{w}_j \, d\bar{x} + \bar{M}_{tp} \bar{v}_i(1) \bar{v}_j(1) = \delta_{ij} M_i \qquad \text{(C11)}$$

Equation (C11) is the first orthogonality condition for the bending modes of a solar array in a 1-g field. A second orthogonality condition can be obtained by dividing equations (C10) and (C9) by $\bar{\beta}_j^4$ and $\bar{\beta}_i^4$, respectively, and subtracting the resulting equations. The result is

$$\frac{\bar{k}^2}{2\bar{P}} \int_1^{\zeta_0} \zeta \frac{d\bar{w}_i}{d\zeta} \frac{d\bar{w}_j}{d\zeta} d\zeta + \int_0^1 \frac{d^2\bar{v}_i}{d\bar{x}^2} \frac{d^2\bar{v}_j}{d\bar{x}^2} d\bar{x} - \bar{k}^2 \int_0^1 \frac{d\bar{v}_i}{d\bar{x}} \frac{d\bar{v}_j}{d\bar{x}} d\bar{x} = \delta_{ij} \bar{\beta}_i^4 M_i \tag{C12}$$

To obtain the orthogonality conditions for the array in a 0-g field, ζ is transformed to $\bar{x}$ by using equation (4) and the limit is taken as W_m approaches zero. The results yield the first and second orthogonality conditions in the following form:

$$\int_0^1 \bar{v}_i \bar{v}_j \, d\bar{x} + \bar{M}_m \int_0^1 \bar{w}_i \bar{w}_j \, d\bar{x} + \bar{M}_{tp} \bar{v}_i(1) \bar{v}_j(1) = \delta_{ij} M_i \tag{C13}$$

$$\bar{k}^2 \int_0^1 \frac{d\bar{w}_i}{d\bar{x}} \frac{d\bar{w}_j}{d\bar{x}} d\bar{x} + \int_0^1 \frac{d^2\bar{v}_i}{d\bar{x}} \frac{d^2\bar{v}_j}{d\bar{x}} d\bar{x} - \bar{k}^2 \int_0^1 \frac{d\bar{v}_i}{d\bar{x}} \frac{d\bar{v}_j}{d\bar{x}} d\bar{x} = \delta_{ij} \bar{\beta}_i^4 M_i \tag{C14}$$

where M_i for this case is given by

$$M_i = \int_0^1 \bar{v}_i^2 \, d\bar{x} + \bar{M}_m \int_0^1 \bar{w}_i^2 \, d\bar{x} + \bar{M}_{tp} \bar{v}_i^2(1) \tag{C15}$$

The orthogonality conditions for the torsional modes can be developed in a manner similar to that used for the bending modes. For the i^{th} mode of vibration, equations (22) to (24) yield the following set of equations and boundary conditions:

$$\frac{d}{d\zeta}\left(\zeta \frac{d\varphi_i}{d\zeta}\right) + 4\beta_{ti}^2 \bar{P} \zeta \varphi_i = 0 \tag{C16}$$

$$\frac{d^2\theta}{d\bar{x}^2} + \bar{I}_b \bar{k}_t^2 \bar{\beta}_{ti}^2 \theta_i = 0 \tag{C17}$$

$$\frac{d\theta_i(1)}{d\bar{x}} - \frac{1}{24} \frac{\bar{k}_t^2}{\bar{P}} \frac{d\varphi_i(1)}{d\zeta} - \bar{I}_{tp} \bar{k}_t^2 \bar{\beta}_{ti}^2 \theta_i(1) = 0 \tag{C18}$$

$$\left.\begin{aligned} \varphi(\zeta_0) &= 0 \\ \theta_i(1) &= \varphi_i(1) \end{aligned}\right\} \tag{C19}$$

$$\theta(0) = 0 \tag{C20}$$

Multiplying equation (C16) by φ_j, integrating over the length, and applying the boundary conditions given by equations (C19) yield

$$\theta_j(1)\frac{d\varphi_i(1)}{d\zeta} + 4\bar{\beta}_{ti}^2\bar{P}\int_{\zeta_0}^{1}\zeta\varphi_i\varphi_j\,d\zeta - \int_{\zeta_0}^{1}\zeta\frac{d\varphi_i}{d\zeta}\frac{d\varphi_j}{d\zeta}\,d\zeta = 0 \tag{C21}$$

Similarly, multiplying equation (C17) by θ_j, integrating over the length, and using equations (C18) and (C20) give

$$\frac{1}{24}\frac{\bar{k}_t^2}{\bar{P}}\theta_j(1)\frac{d\varphi_i(1)}{d\zeta} - \int_0^1\frac{d\theta_i}{d\bar{x}}\frac{d\theta_j}{d\bar{x}}\,d\bar{x} + \bar{\beta}_{ti}^2\bar{k}_t^2\left[\int_0^1\theta_i\theta_j\,d\bar{x} + \bar{I}_{tp}\theta_i(1)\theta_j(1)\right] = 0 \tag{C22}$$

Now multiply equation (C21) by $\bar{k}_t^2/24\bar{P}$ and subtract from equation (C22) to obtain

$$-\int_0^1\frac{d\theta_i}{d\bar{x}}\frac{d\theta_j}{d\bar{x}}\,d\bar{x} - \frac{\bar{k}_t^2}{24\bar{P}}\int_1^{\zeta_0}\zeta\frac{d\varphi_i}{d\zeta}\frac{d\varphi_j}{d\zeta}\,d\zeta + \bar{\beta}_{ti}^2\bar{k}_t^2\left[\bar{I}_b\int_0^1\theta_i\theta_j\,d\bar{x} - \frac{\bar{P}}{6}\int_1^{\zeta_0}\zeta\varphi_i\varphi_j\,d\zeta + \bar{I}_{tp}\theta_i(1)\theta_j(1)\right] = 0 \tag{C23}$$

Interchanging i and j in equation (C23) yields

$$- \int_0^1 \frac{d\theta_i}{d\bar{x}} \frac{d\theta_j}{d\bar{x}} d\bar{x} - \frac{\bar{k}_t^2}{24\bar{P}} \int_1^{\zeta_0} \zeta \frac{d\varphi_i}{d\zeta} \frac{d\varphi_j}{d\zeta} d\zeta$$

$$+ \bar{\beta}_{tj}^2 \bar{k}_t^2 \left[\bar{I}_b \int_0^1 \theta_i \theta_j \, d\bar{x} - \frac{\bar{P}}{6} \int_1^{\zeta_0} \zeta \varphi_i \varphi_j \, d\zeta + \bar{I}_{tp} \theta_i(1) \theta_j(1) \right] = 0 \qquad \text{(C24)}$$

Subtracting equation (24) from equation (23) yields the first orthogonality condition for the torsional modes of the solar array in a 1-g field. Thus,

$$\bar{I}_b \int_0^1 \theta_i \theta_j \, d\bar{x} + \frac{\bar{P}}{6} \int_1^{\zeta_0} \zeta \varphi_i \varphi_j \, d\zeta + \bar{I}_{tp} \theta_i(1) \theta_j(1) = \delta_{ij} T_i \qquad \text{(C25)}$$

where T_i is the generalized mass defined by

$$T_i = I_b \int_0^1 \theta_i^2 \, d\bar{x} + \frac{\bar{P}}{6} \int_1^{\zeta_0} \zeta \varphi_i^2 \, d\zeta + \bar{I}_{tp} \theta_i^2(1) \qquad \text{(C26)}$$

Similarly, the second orthogonality condition for this case is obtained by dividing equations (C24) and (C23) by $\bar{\beta}_{tj}^2$ and $\bar{\beta}_{ti}^2$, respectively, and subtracting the resulting equations. The results can be expressed as

$$\int_0^1 \frac{d\theta_i}{d\bar{x}} \frac{d\theta_j}{d\bar{x}} d\bar{x} + \frac{\bar{k}_t^2}{24\bar{P}} \int_1^{\zeta_0} \zeta \frac{d\varphi_i}{d\zeta} \frac{d\varphi_j}{d\zeta} d\bar{x} = \delta_{ij} \bar{k}_t^2 \bar{\beta}_{ti}^2 T_i \qquad \text{(C27)}$$

Finally, the orthogonality relations for the 0-g configuration can be obtained by equations (C25) and (C26) by using equation (4) to transform ζ into $\bar{x}$ and taking the limit as W_m approaches zero (i.e., $\bar{P} \to \infty$). The results are

$$\bar{I}_b \int_0^1 \theta_i \theta_j \, d\bar{x} + \frac{1}{12} \int_0^1 \varphi_i \varphi_j \, d\bar{x} + \bar{I}_{tp} \theta_i(1) \theta_j(1) = \delta_{ij} T_i \qquad \text{(C28)}$$

$$\int_0^1 \frac{d\theta_i}{d\bar{x}} \frac{d\theta_j}{d\bar{x}} d\bar{x} + \frac{\bar{k}_t^2}{12} \int_0^1 \frac{d\varphi_i}{d\bar{x}} \frac{d\varphi_j}{d\bar{x}} d\bar{x} = \delta_{ij} \bar{k}_t^2 \bar{\beta}_{ti}^2 T_i \qquad \text{(C29)}$$

where T_i in equations (C28) and (C29) is given by

$$T_i = I_b \int_0^1 \theta_i^2 \, d\bar{x} + \frac{1}{12} \int_0^1 \varphi_i^2 \, d\bar{x} + \bar{I}_{tp} \theta_i^2(1)$$

APPENDIX D

SYMBOLS

A, B, C, A_1, B_1, C_1	arbitrary constants of integration
A_2, B_2, C_2	constants defined by eq. (81) or (84)
b	blanket width
$\bar{b}$	nondimensional blanket width, b/ℓ
b_{mn}	elements of stiffness matrix defined by eq. (62)
EI	boom bending stiffness
G_{mn}	element of mass matrix defined by eq. (65)
I_b	mass polar moment of inertia per unit length of boom
I_{tp}	mass moment of inertia of tip piece about its center of gravity
$\bar{I}_b$	boom inertia ratio, $I_b/P_m b^2$
$\bar{I}_{tp}$	tip-piece inertia ratio, $I_{tp}/M_m b^2$
JG	boom torsional stiffness
K_{mn}	element of stiffness matrix defined by eq. (61)
$[\bar{K}]$	nondimensional stiffness matrix
$[\bar{K}^{ij}]$	i^{th}, j^{th} submatrix of the stiffness matrix $\bar{K}$
$\bar{k}$	axial load parameter for bending, $\sqrt{P\ell^2/EI}$
$\bar{k}_t$	torsional stiffness factor, $\sqrt{Pb^2/JG}$
ℓ	blanket and boom length
M_b	total mass of boom, $\rho_b \ell$
M_i	i^{th} generalized mass of solar array for bending
M_m	total blanket mass, $\rho_m \ell$
M_{tp}	mass of tip piece
$M_x(x)$	torsional moment distribution along boom
$M_y(x)$	bending moment distribution along boom
$\bar{M}_m$	mass ratio, M_m/M_b
$\bar{M}_{tp}$	mass ratio, M_{tp}/M_b

$[\overline{M}]$	nondimensional mass matrix
$[\overline{M}^{ij}]$	i^{th}, j^{th} submatrix of mass matrix $\overline{M}$
$N_x^{(0)}$	uniform stress resultant in blanket at rest
P	compressive preload in boom
$\overline{P}$	ratio of axial load to blanket weight, P/W_m
P_{cr}	critical buckling load of array
$P_{cr,0}$	critical buckling load of array in 0-g configuration
$Q(x)$	shear distribution along boom
$q_n(t)$	n^{th} generalized coordinate
$\{q\}$	column matrix of generalized coordinates
T	blanket tension per unit width
T_b	kinetic energy function of boom
T_i	i^{th} generalized mass of solar array for torsion
T_m	kinetic energy function of blanket
T_T	total kinetic energy of array
T_{tp}	kinetic energy of tip piece
U	total strain of array
U_b	strain energy function for boom
U_m	strain energy function for blanket
$V(x,y,t), v(x)$	boom displacement
$\overline{V}, \overline{v}(\overline{x})$	nondimensional boom displacement, V/ℓ and v/ℓ
W_m	total blanket weight, $\rho_m g \ell$
$W(x,y,t), w(x)$	blanket displacement
$\overline{W}, \overline{w}(\overline{x})$	nondimensional blanket displacement, W/ℓ and w/ℓ
x	longitudinal coordinate of blanket and boom
$\overline{x}$	nondimensional longitudinal coordinate
y	lateral coordinate of blanket
α_{cn}	n^{th} modal parameter for uniform cantilevered beam
$\alpha_1, \alpha_2, \alpha_3$	characteristic values, eqs. (27) and (41)
$\overline{\beta}$	bending frequency parameter, $\sqrt[4]{(M_b \ell^3/EI)\omega^2}$

$\bar{\beta}_{cn}$	n^{th} natural frequency for uniform cantilevered beam
$\bar{\beta}_{d1}$	first natural bending frequency parameter for uniform beam under directed axial load
$\bar{\beta}_n$	n^{th} natural bending frequency parameter
$\bar{\beta}_t$	torsional frequency parameter
$\bar{\beta}_{tn}$	n^{th} natural torsional frequency parameter
δ_{mn}	Kronecker delta function
ζ	transformed coordinate defined by eq. (4)
ζ_0	transformed coordinate at point $x = 0$
$\bar{\eta}_n(\bar{x})$	n^{th} assumed function for boom
$\theta(x,t), \theta(x)$	rotation of boom cross section
κ_1	bending parameter, $\bar{P}/\bar{k}\sqrt{\bar{M}_m}$
κ_2	torsion parameter, $\bar{\beta}_t\bar{P}$
ρ_b	mass per unit length of boom
ρ_m	mass per unit length of blanket
$\varphi(\zeta)$	torsional displacement function
ω	circular frequency of vibration
ω_{cn}	n^{th} natural circular frequency of uniform cantilevered beam
ω_{d1}	first natural frequency of uniform cantilevered beam under directed axial load
ω_n	n^{th} natural circular frequency of vibration

Subscripts:

$'$	differentiation with respect to $\bar{x}$
$\cdot$	differentiation with respect to time $\bar{t}$

REFERENCES

1. Likens, P. W.: Dynamics and Control of Flexible Space Vehicles. (JPL-TR-32-1329, Jet Propulsion Lab.; NAS7-100) NASA CR-105592, 1969.

2. Hughes, P. C.: Attitude Dynamics of a Three Axis Stabilized Satellite with a Large Flexible Solar Array. AIAA Paper 72-857, Aug. 1972.

3. Harrison, T. D.: Communications Technology Satellite Deployed Solar Array Dynamics Tests. CRC-1264, Communications Research Centre, 1975.

4. Shepard, N. F., et al.: Design and Development of a 30-Watt-per-Pound, 250 Square Foot Roll-Up Solar Array. Document 70 SD 4286, General Electric Co., 1970.

5. Hughes, P. C.; and Gary, S. C.: Dynamics of Large Flexible Solar Arrays and Application to Spacecraft Attitude Control System Design. UTIAS-179, Toronto Univ., 1963.

6. Coyner, J. V., Jr.; and Ross, R. G., Jr.: Parametric Study of the Performance Characteristics and Weight Variations of Large-Area Roll-Up Solar Arrays. (JPL-TR-32-1502, Jet Propulsion Lab.; NAS7-100) NASA CR-115821, 1970.

7. Vigneron, F.: A Structural Dynamics Model for Flexible Solar Array of the Communications Technology Satellite. CRC-1268, Communications Research Centre, 1975.

8. Shaker, Francis J.: Effect of Axial Load on Mode Shapes and Frequencies of Beams. NASA TN D-8109, 1975.

9. Merrovitch, Leonard: Analytical Methods in Vibration. The MacMillan Co., 1967.

10. McLachlan, Norman W.: Bessel Functions for Engineers. Oxford University Press, 1961.

11. Timoshenko, Stephen P.; and Gere, James M.: Theory of Elastic Stability. McGraw-Hill Book Co., Inc., 1961.

12. Bleich, Freidrich: Buckling Strength of Metal Structures. McGraw-Hill Book Co., Inc., 1952.

13. Bishop, Richard E. D.; Gladwell, G. M. L.; and Michaelson, S.: The Matrix Analysis of Vibration. Cambridge University Press, 1965.

14. Young, D.; and Felgar, R. P., Jr.: Tables of Characteristic Functions Representing Normal Modes of Vibration of a Beam. Publ. No. 4913, Univ. Texas, 1949.

15. Ralston, Anthony: A First Course in Numerical Analysis. McGraw-Hill Book Co., Inc., 1965.

TABLE I. - VALUES OF $\overline{\beta}_{cn}$ AND α_{cn}

FROM REFERENCE 14

n	n^{th} natural torsional frequency parameter, $\overline{\beta}_{cn}$	n^{th} modal parameter for uniform beam, α_{cn}	Remarks
1	1.87510407	0.7340955	For $n > 5$
2	4.69509113	1.01846644	$\beta_{cn} \approx (2n - 1)\left(\frac{\pi}{2}\right)$
3	7.85475743	.99922450	$\alpha_n \approx 1$
4	10.99554074	1.000033553	
5	14.13716839	.9999985501	
6	$11\left(\frac{\pi}{2}\right)$	1	
7	$13\left(\frac{\pi}{2}\right)$	↓	
8	$15\left(\frac{\pi}{2}\right)$		
9	$17\left(\frac{\pi}{2}\right)$		
10	$19\left(\frac{\pi}{2}\right)$		

TABLE II. - STRUCTURAL DYNAMIC CHARACTERISTICS OF CANTILEVERED BEAM UNDER AXIAL LOAD DIRECTED THROUGH ROOT

Axial load ratio, $P/P_{cr,0}$	Tip displacement, $\overline{\eta}_1(1)$	Generalized mass, $\int_0^1 \eta_1^2(\zeta)d\zeta$	Frequency parameter, $\overline{\beta}_{d1}$
0	2.00	1.00	1.875104069
.001	2.000687704	1.000542243	1.874861498
.01	2.007105600	1.005646573	1.872665819
.02	2.014727517	1.011801344	1.870199290
.04	2.031574652	1.025702328	1.865178790
.06	2.050653505	1.041844802	1.860037145
.08	2.072081985	1.060384811	1.854768565
.10	2.095984442	1.081494411	1.849366860
.20	2.257519322	1.233025493	1.820112101
.30	2.505117303	1.488716586	1.786295523
.40	2.870244314	1.910797481	1.746376307
.50	3.407887443	2.624651093	1.697963692
.60	4.227974273	3.919604287	1.637089120
.70	5.588861642	6.609907291	1.556494718
.80	8.269873146	13.874364178	1.440685832
.90	16.176957259	50.465329261	1.244925094
.93	22.906582764	99.461655188	1.148904957
.96	39.687051208	293.170363886	1.008218686
.98	78.7905575842	1140.85733402	.853258066
1.00	∞	∞	0

TABLE III. - COMPARISON BETWEEN EXACT SOLUTION AND RAYLEIGH-RITZ SOLUTION FOR BENDING FREQUENCIES OF SOLAR ARRAY IN 0-g FIELD

[Ratio of blanket mass to total boom mass, $\overline{M}_m$, 3.0; ratio of tip-piece mass to total boom mass, $\overline{M}_{tp}$, 1.0.]

(a) Fundamental bending frequency

Axial load ratio, $P/P_{cr,0}$	Exact-solution equation	Rayleigh-Ritz solution using cantilevered beam modes						Two-mode Rayleigh-Ritz solution (eq. (80))	
		N=3, M=3	Error, percent	N=4, M=4	Error, percent	N=5, M=5	Error, percent	N=1, M=1	Error, percent
0.001	0.42378	0.42378	0	0.42378	0	0.42378	0	0.42380	0.005
.01	.74051	.74054	.004	.74053	.003	.74052	.001	.74105	.073
.02	.85891	.85906	.012	.85901	.006	.85899	.003	.86063	.195
.04	.96058	.96085	.028	.96070	.012	.96064	.006	.96495	.455
.06	.99854	.99893	.039	.99871	.017	.99863	.009	1.0045	.597
.08	1.0149	1.0153	.039	1.0151	.020	1.0150	.010	1.0214	.640
.10	1.0224	1.0229	.049	1.0226	.020	1.0225	.010	1.0291	.655
.20	1.0225	1.0231	.059	1.0227	.020	1.0226	.010	1.0289	.626
.30	1.0052	1.00607	.087	1.0055	.030	1.0054	.020	1.0112	.597
.40	.98085	.98206	.123	.98125	.041	.98110	.025	.98631	.557
.50	.95009	.95179	.179	.95066	.060	.95044	.037	.95496	.513
.60	.91133	.91380	.271	.91216	.091	.91184	.056	.91550	.458
.70	.86086	.86462	.437	.86217	.152	.86166	.093	.86419	.387
.80	.79049	.79670	.786	.79274	.285	.79183	.170	.79280	.292
.90	.67648	.68909	1.86	.68132	.715	.67929	.415	.67760	.166
.93	.62223	.63954	2.78	.62905	1.10	.62616	.632	.62298	.121
.96	.54412	.57128	4.99	.55520	2.04	.55049	1.17	.54451	.072
.98	.45935	.50382	9.68	.47842	4.15	.47038	2.40	.45952	.037

(b) Second bending frequency

0.001	0.59928	0.59928	0	0.59928	0	0.59928	0	1.1730	95.7
.01	1.0349	1.0353	.039	1.0351	.019	1.0350	.010	1.1912	15.1
.02	1.1559	1.1573	.121	1.1565	.052	1.1562	.026	1.2178	5.35
.04	1.2606	1.2619	.103	1.2612	.048	1.2609	.024	1.2873	2.12
.06	1.3463	1.3472	.067	1.3467	.030	1.3465	.015	1.3639	1.31
.08	1.4225	1.4233	.056	1.4228	.021	1.4227	.014	1.4363	.970
.10	1.4900	1.4907	.047	1.4903	.020	1.4902	.013	1.5019	.799
.20	1.7424	1.7430	.034	1.7427	.017	1.7426	.011	1.7516	.528
.30	1.9188	1.9194	.031	1.9191	.016	1.9190	.010	1.9278	.469
.40	2.0571	2.0576	.024	2.0573	.010	2.0572	.005	2.0664	.452
.50	2.1721	2.1727	.028	2.1724	.014	2.1722	.005	2.1819	.451
.60	2.2713	2.2719	.026	2.2716	.013	2.2715	.009	2.2817	.458
.70	2.3590	2.3596	.025	2.3593	.013	2.3591	.004	2.3702	.475
.80	2.4378	2.4385	.029	2.4381	.012	2.4380	.008	2.4500	.500
.90	2.5097	2.5103	.024	2.5100	.012	2.5098	.004	2.5229	.526
.93	2.5300	2.5307	.028	2.5304	.016	2.5302	.008	2.5436	.538
.96	2.5499	2.5506	.027	2.5503	.016	2.5501	.008	2.5639	.549
.98	2.5629	2.5636	.027	2.5633	.016	2.5631	.008	2.5772	.558

(c) Third bending frequency

0.001	0.73387	0.73388	0.001	0.73387	0	0.73387	0	-------	------
.01	1.2127	1.2177	.412	1.2146	.157	1.2137	.082	-------	------
.02	1.3489	1.3517	.208	1.3501	.089	1.3495	.044	-------	------
.04	1.5681	1.5696	.096	1.5687	.038	1.5684	.019	-------	------
.06	1.7267	1.7279	.069	1.7272	.029	1.7270	.017	-------	------
.08	1.8515	1.8526	.059	1.8520	.027	1.8518	.016	-------	------
.10	1.9554	1.9565	.056	1.9559	.026	1.9556	.010	-------	------
.20	2.3202	2.3213	.047	2.3206	.017	2.3204	.009	-------	------
.30	2.5656	2.5668	.047	2.5661	.019	2.5659	.012	-------	------
.40	2.7555	2.7568	.047	2.7560	.018	2.7558	.011	-------	------
.50	2.9122	2.9136	.048	2.9128	.021	2.9125	.010	-------	------
.60	3.0462	3.0477	.049	3.0468	.020	3.0465	.010	-------	------
.70	3.1630	3.1647	.054	3.1638	.025	3.1634	.013	-------	------
.80	3.2643	3.2665	.067	3.2654	.034	3.2648	.015	-------	------
.90	3.3411	3.3464	.159	3.3441	.090	3.3424	.039	-------	------
.93	3.3525	3.3606	.242	3.3573	.143	3.3547	.066	-------	------
.96	3.3542	3.3661	.355	3.3613	.212	3.3573	.092	-------	------
.98	3.3498	3.3641	.427	3.3583	.254	3.3535	.110	-------	------

TABLE IV. - COMPARISON BETWEEN EXACT SOLUTION AND RAYLEIGH-RITZ SOLUTION FOR BENDING FREQUENCIES OF SOLAR ARRAY IN A 1-g FIELD

[Ratio of blanket mass to total boom mass, $\overline{M}_m$, 3.0; ratio of tip-piece mass to total boom mass, $\overline{M}_{tp}$, 1.0; ratio of array 0-g critical buckling load to total blanket weight, $P_{cr,0}/W_m$, 1.0.]

(a) Fundamental bending frequency

Axial-load ratio, $P/P_{cr,0}$	Exact-solution equation	Rayleigh-Ritz solution					
		N=3, M=3	Error, percent	N=5, M=5	Error, percent	N=10, M=10	Error, percent
0.001	1.3261	1.3445	1.387	1.3416	1.169	1.3379	0.890
.050	1.3433	1.3453	.149	1.3442	.067	1.3436	.022
.10	1.3431	1.3439	.060	1.3433	.015	1.3431	0
.20	1.3376	1.3380	.030	1.3378	.015	1.3377	.007
.40	1.3196	1.3201	.038	1.3197	.008	1.3196	0
.60	1.2944	1.2952	.062	1.2946	.015	1.2944	0
.80	1.2599	1.2613	.111	1.2602	.024	1.2599	0
1.00	1.2096	1.2124	.231	1.2103	.058	1.2097	.008
1.20	1.1264	1.1327	.559	1.1279	.133	1.1266	.018
1.40	.94022	.96197	2.313	.94584	.598	.94102	.085
1.517	.35994	.61340	70.4	.47149	31.0	.38301	6.41

(b) Second bending frequency

0.001	1.6858	1.9045	12.97	1.8534	9.94	1.8002	6.79
.050	1.9662	2.0073	2.09	1.9840	.905	1.9706	.224
.10	2.0755	2.0926	.824	2.0810	.265	2.0764	.043
.20	2.2236	2.2281	.202	2.2246	.045	2.2237	.004
.40	2.4263	2.4269	.025	2.4264	.004	2.4263	0
.60	2.5776	2.5778	.008	2.5776	0	2.5776	0
.80	2.7021	2.7023	.007	2.7022	.004	2.7021	0
1.00	2.8088	2.8093	.018	2.8090	.007	2.8089	.004
1.20	2.9008	2.9020	.041	2.9012	.014	2.9009	.003
1.40	2.9349	2.9524	.596	2.9400	.174	2.9357	.027
1.517	2.8131	2.8477	1.230	2.8225	.334	2.8146	.053

(c) Third bending frequency

0.001	2.3892	2.7145	13.6	2.6037	8.98	2.5172	5.36
.050	2.6878	2.8050	4.36	2.7305	1.59	2.6964	.320
.10	2.8219	2.8896	2.40	2.8390	.606	2.8240	.074
.20	3.0104	3.0390	.950	3.0145	.136	3.0107	.010
.40	3.2729	3.2803	.226	3.2733	.012	3.2729	0
.60	3.4606	3.4649	.124	3.4612	.017	3.4607	.003
.80	3.5027	3.5190	.465	3.5066	.111	3.5033	.017
1.00	3.3704	3.3910	.611	3.3756	.154	3.3712	.024
1.20	3.1983	3.2221	.744	3.2045	.194	3.1992	.028
1.40	3.0358	3.0492	.441	3.0390	.105	3.0362	.013
1.517	3.0540	3.0556	.052	3.0545	.016	3.0541	.003

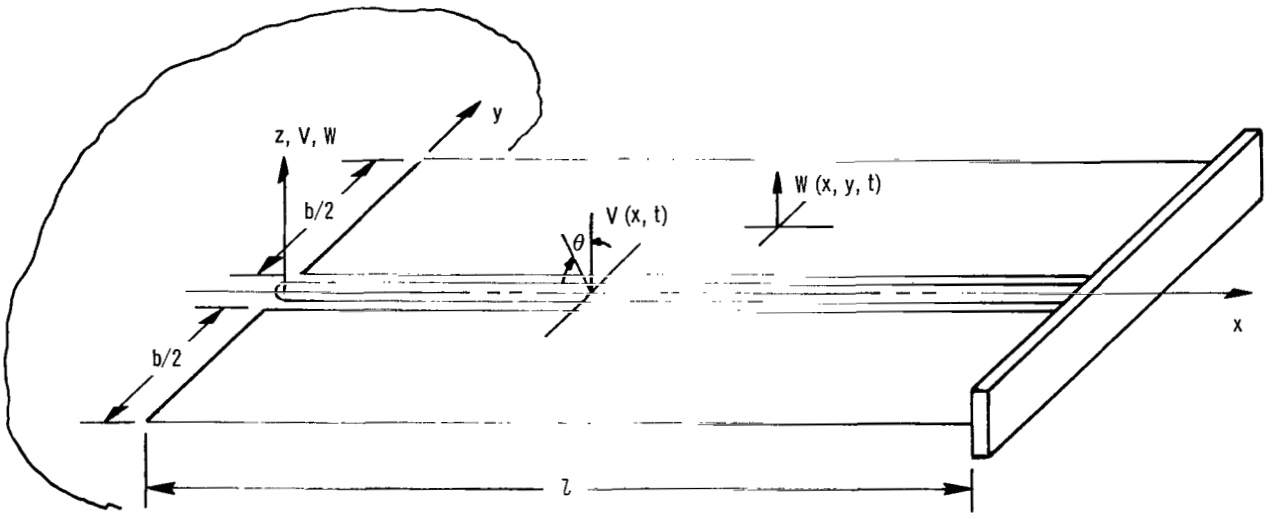

Figure 1. - Geometry and coordinate system for a large solar array with a split blanket.

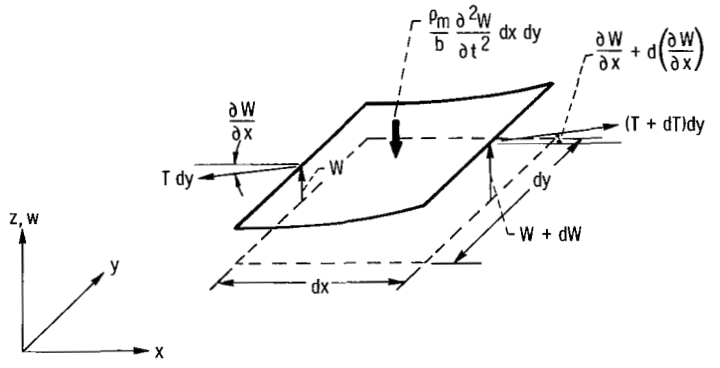

(a) Blanket element showing forces and displacements.

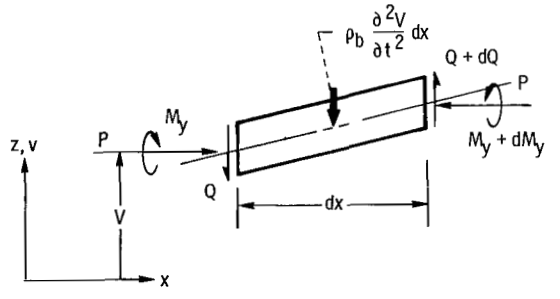

(b) Beam element showing forces, moments, and displacements.

Figure 2. - Forces acting on blanket and beam.

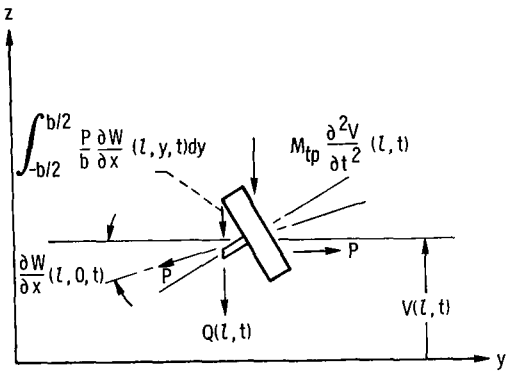

(a) Forces and displacement of tip piece in x-z plane.

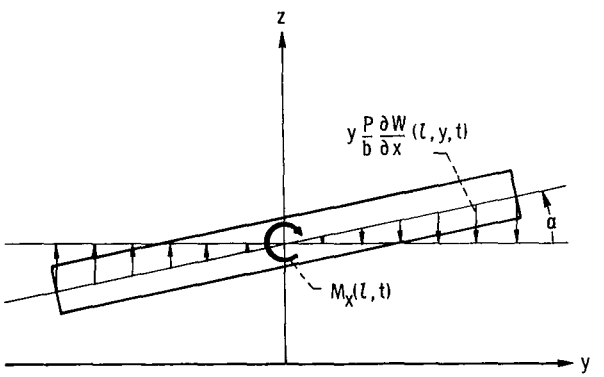

(b) Forces and displacements of tip piece in y-z plane. (For clarity the uniform load $(P/b)\,\partial W/\partial x\,(\ell, t)$ is not shown.)

Figure 3. - Forces and displacements of tip piece.

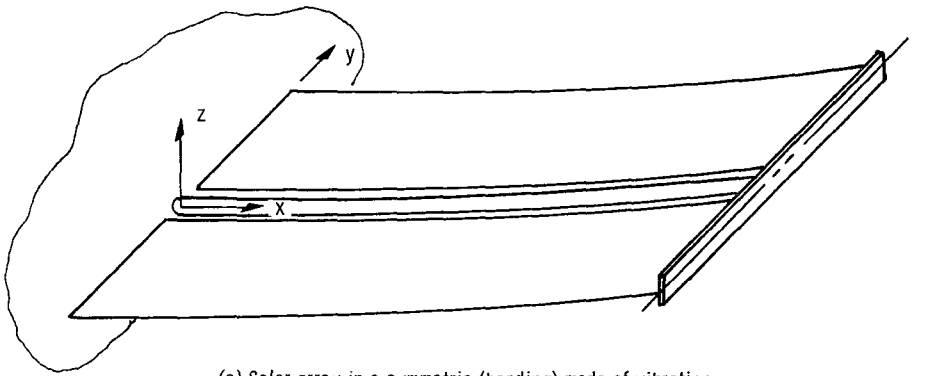

(a) Solar array in a symmetric (bending) mode of vibration.

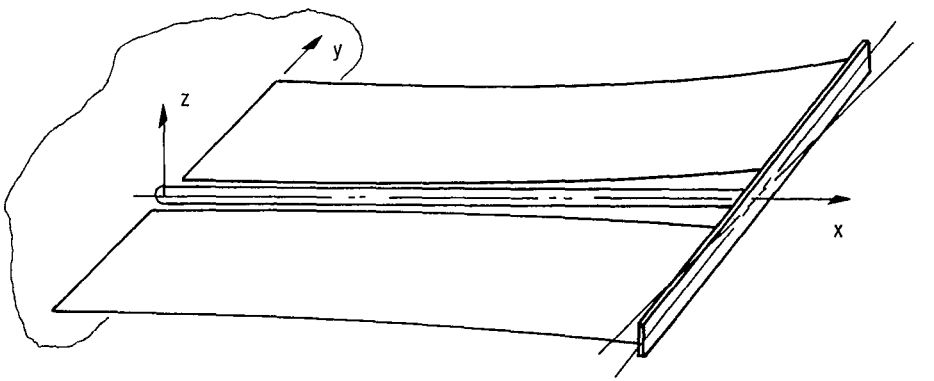

(b) Solar array in an antisymmetric (torsional) mode of vibration.

Figure 4. - Bending and torsional modes of vibration.

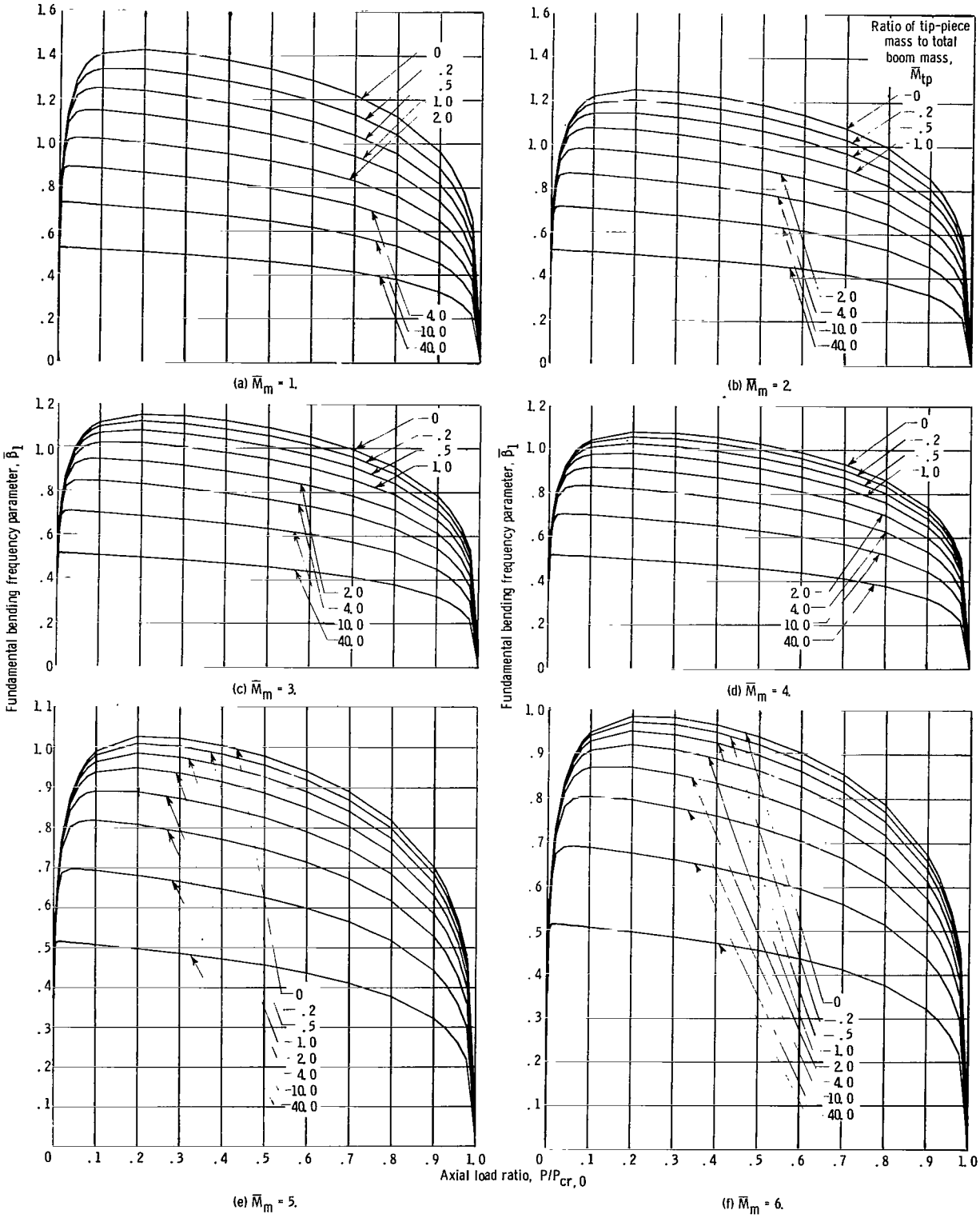

Figure 5. - Fundamental bending frequency as function of axial load for solar array in 0-g field, for various ratios of total blanket mass to total boom mass $\bar{M}_m$.

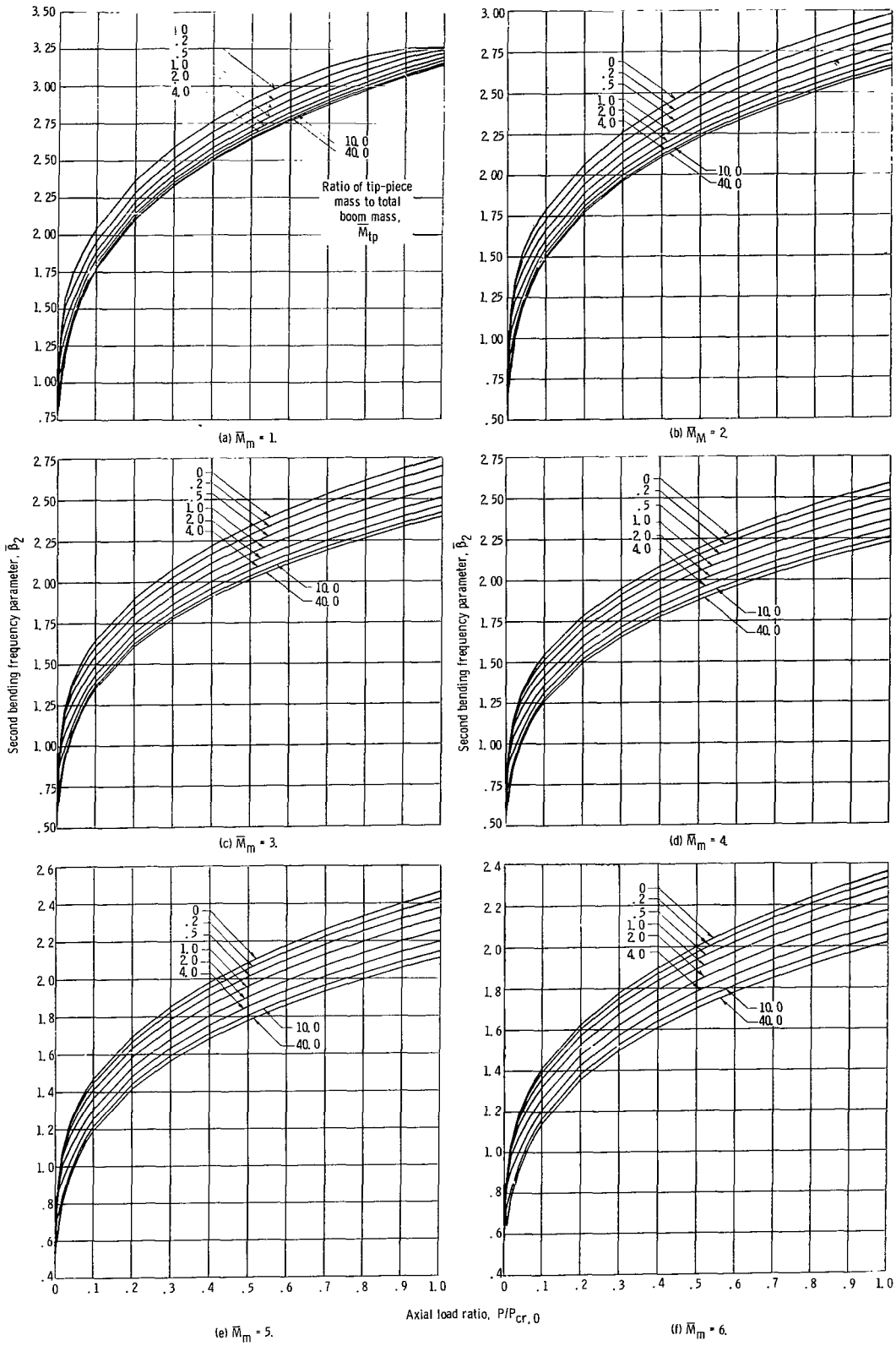

Figure 6. - Second bending frequency as function of axial load for solar array in 0-g field, for various ratios of total blanket mass to total boom mass $\bar{M}_m$.

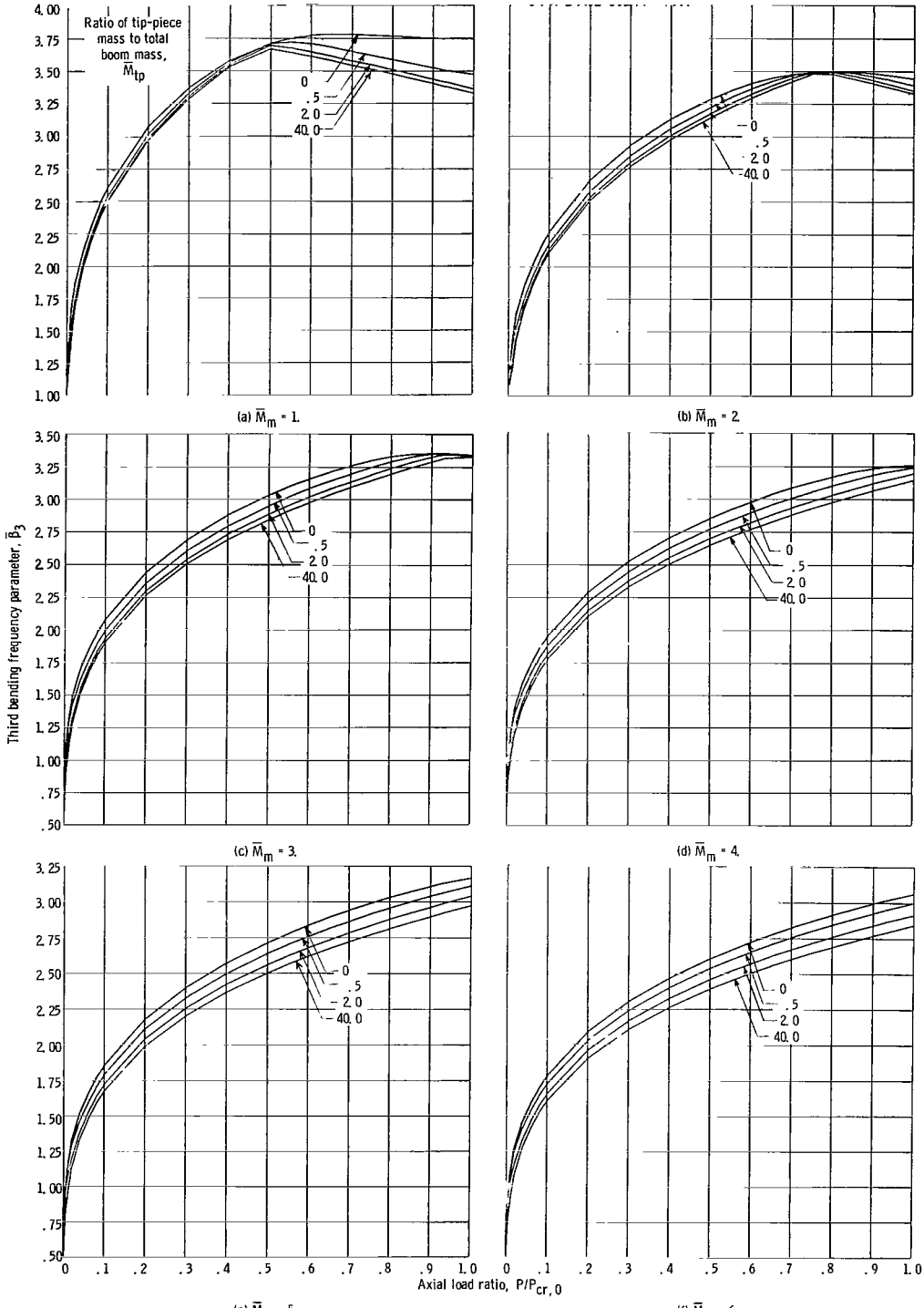

Figure 7. - Third bending frequency as function of axial load for solar array in 0-g field, for various ratios of total blanket mass to total boom mass $\bar{M}_m$.

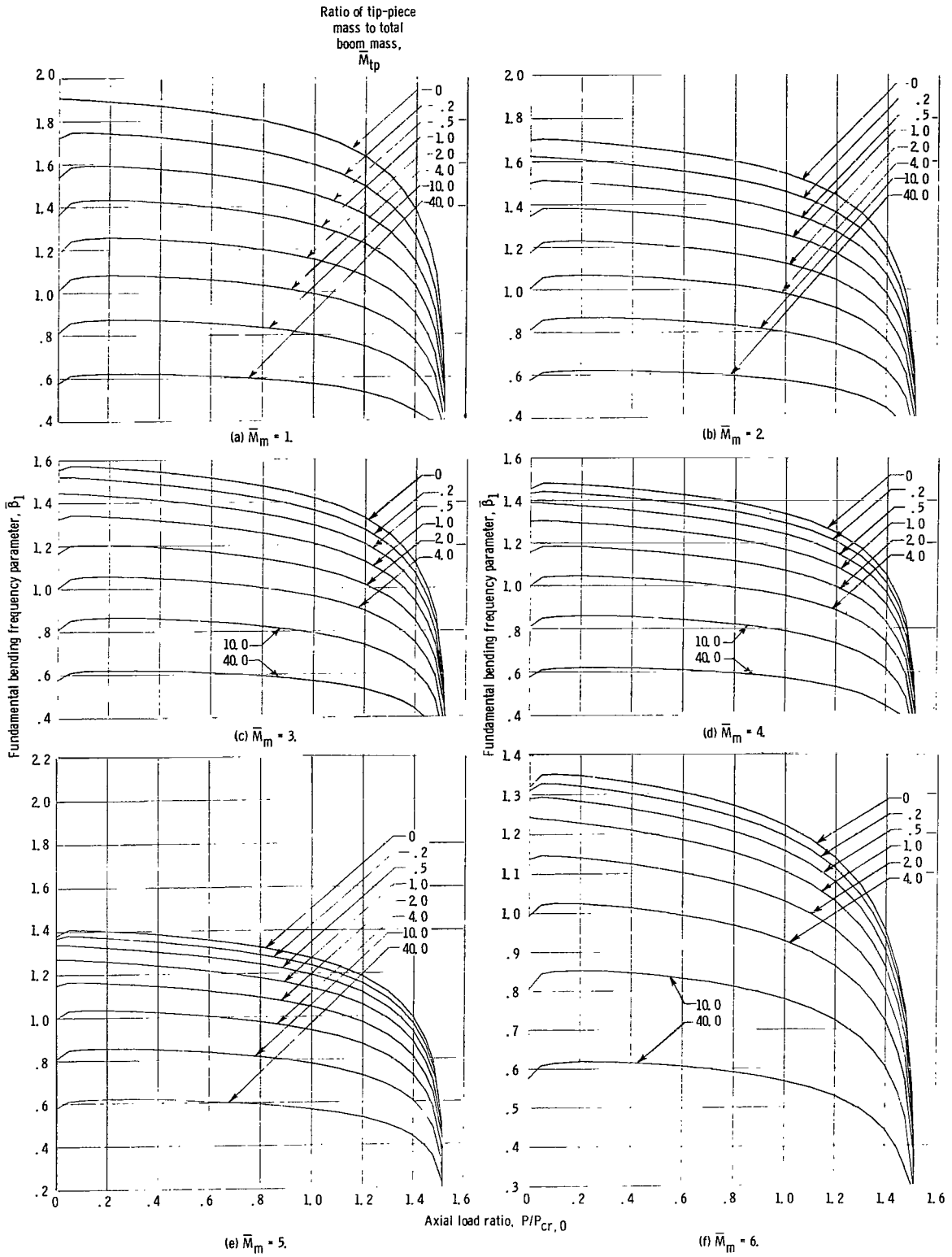

Figure 8. - Fundamental bending frequency as function of axial load for solar array in 1-g field, for various ratios of total blanket mass to total boom mass $\bar{M}_m$. Ratio of array 0-g critical buckling load to total blanket weight, $P_{cr,0}/W_m$, 1.0.

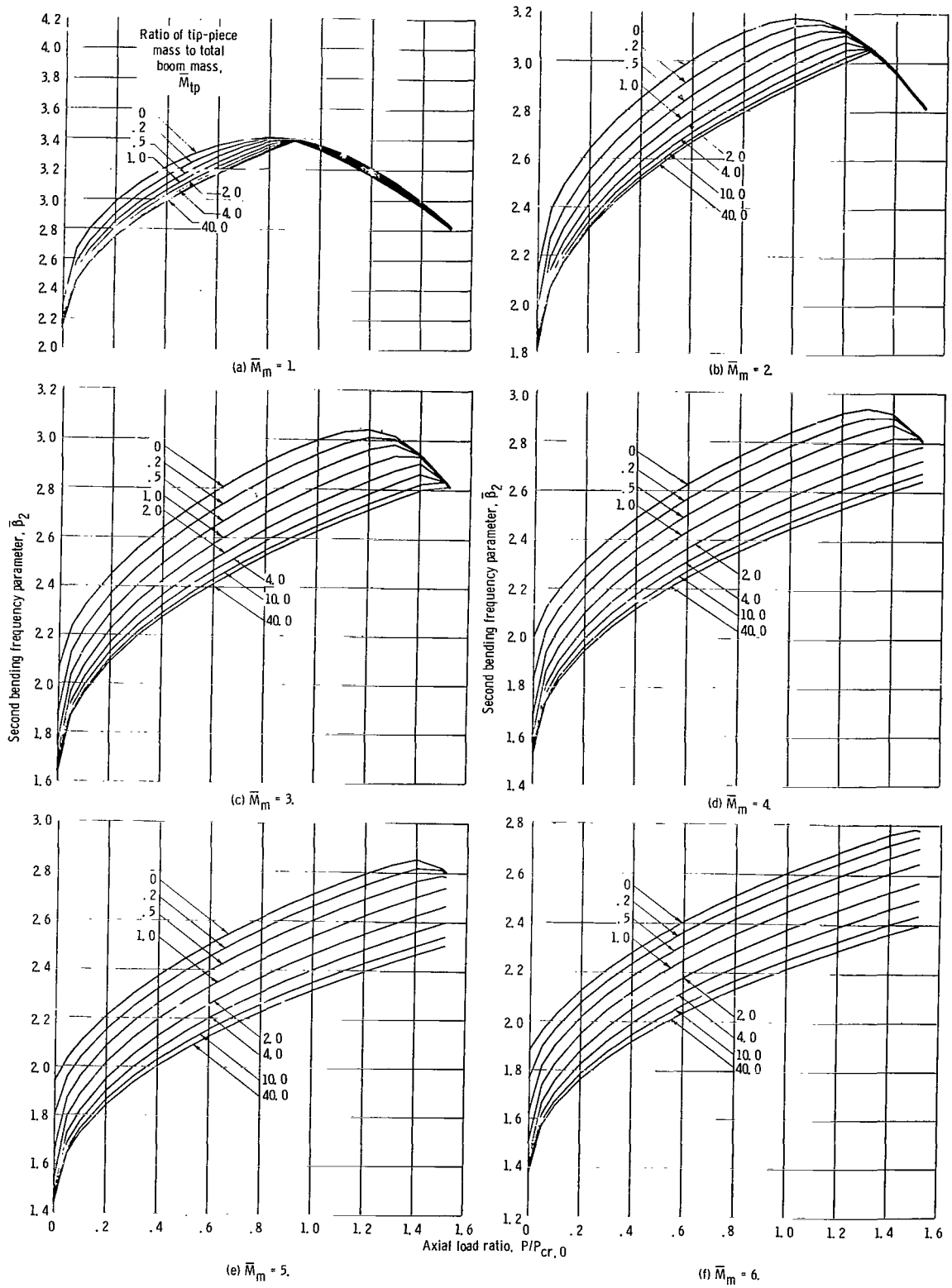

Figure 9. - Second bending frequency as function of axial load for solar array in 1-g field, for various ratios of total blanket mass to total boom mass $\bar{M}_m$. Ratio of array 0-g critical buckling load to total blanket weight, $P_{cr,0}/W_m$, 1.0.

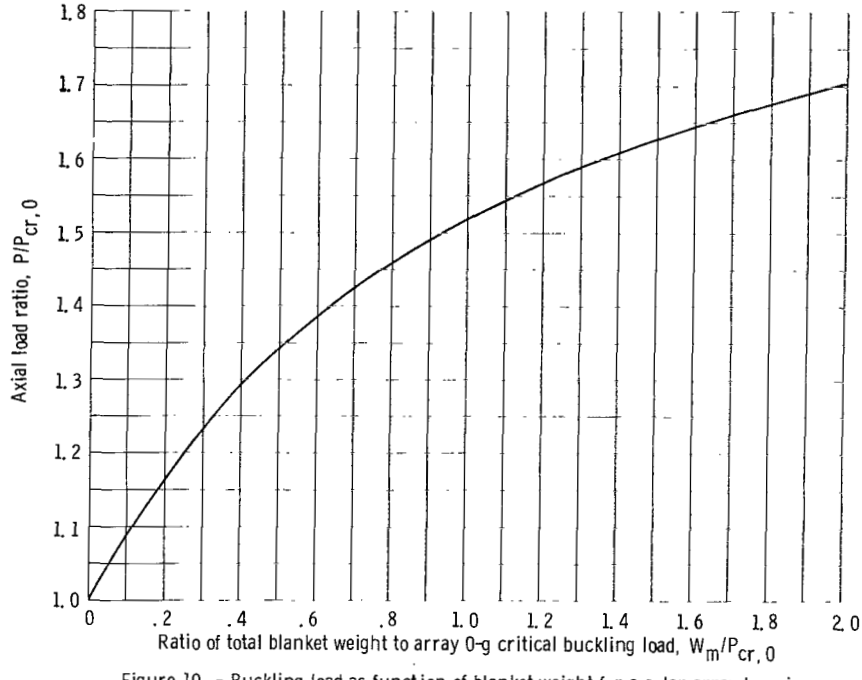

Figure 10. - Buckling load as function of blanket weight for a solar array hanging vertically in 1-g field.

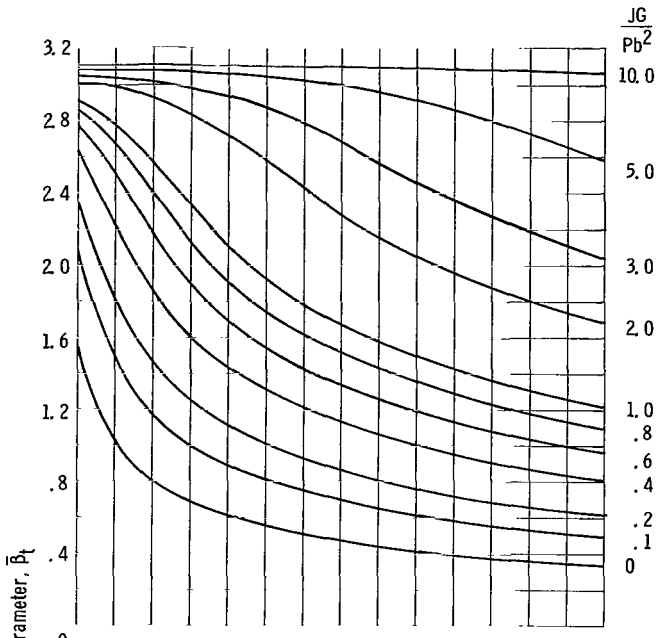

(a) Fundamental torsional frequency.

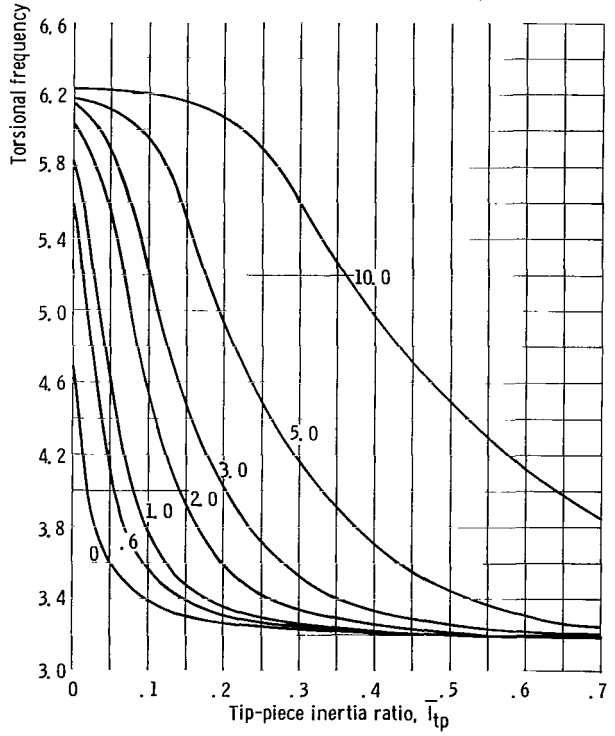

(b) Second torsional frequency.

Figure 11. - Torsional frequency as function of tip-piece inertia for split-blanket solar array in 0-g field.

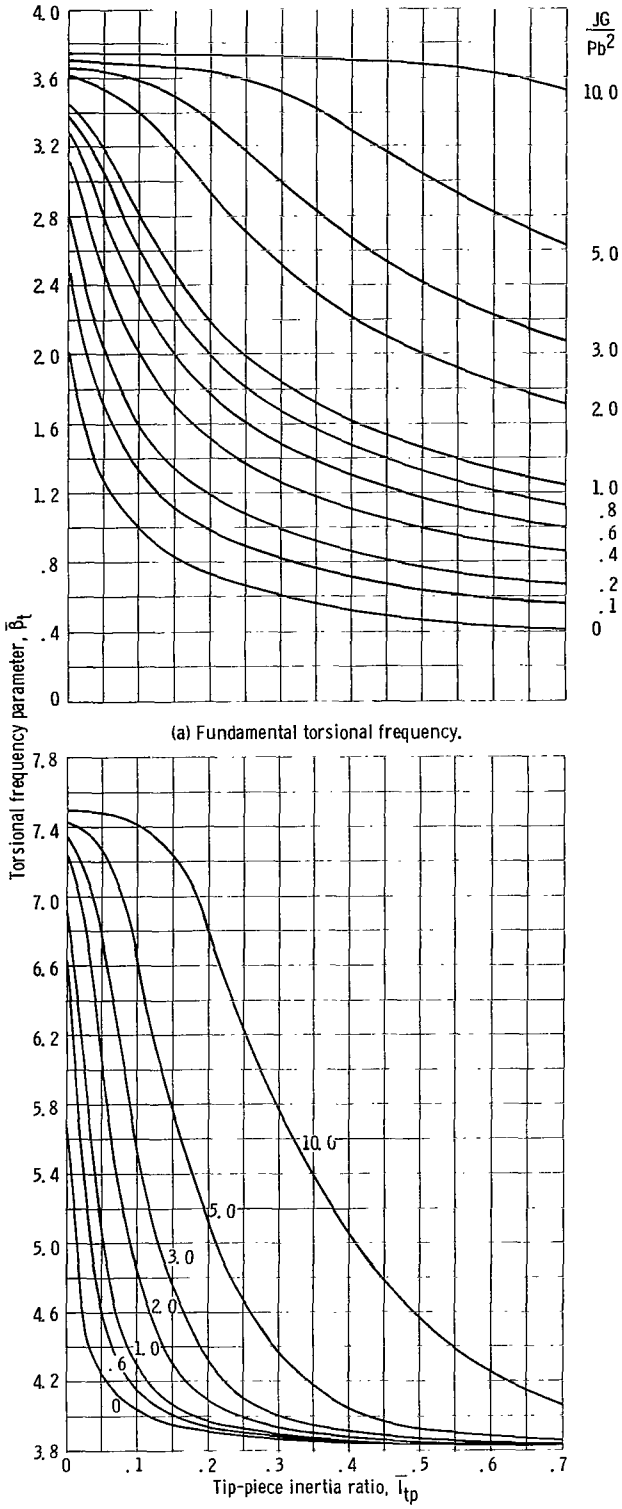

Figure 12. - Torsional frequency as function of tip-piece inertia for split-blanket solar array in 1-g field. Ratio of array 0-g critical buckling load to total blanket weight, $P_{cr,0}/W_m$, 1.0.

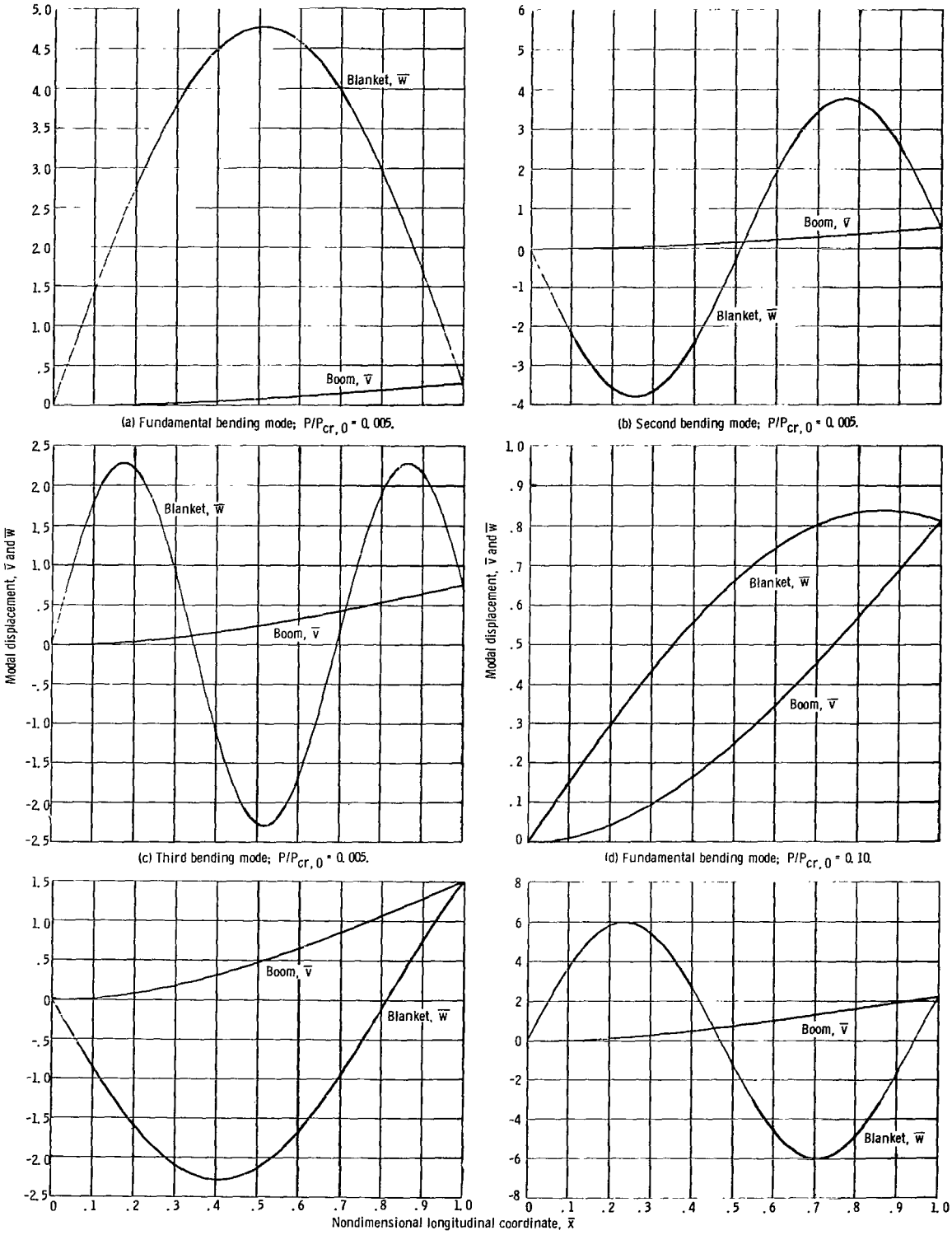

Figure 13. - Bending mode shapes of solar array in 0-g field as function of axial load ratio $P/P_{cr,0}$. Ratio of total blanket mass to total boom mass, $\bar{M}_m$, 3.0; ratio of tip-piece mass to total boom mass, $\bar{M}_{tp}$, 1.0.

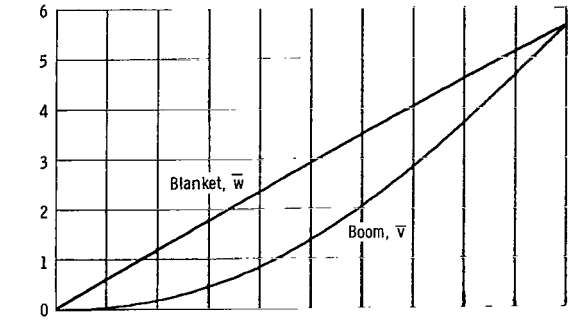

(g) Fundamental bending mode; $P/P_{cr,0} = 0.70$.

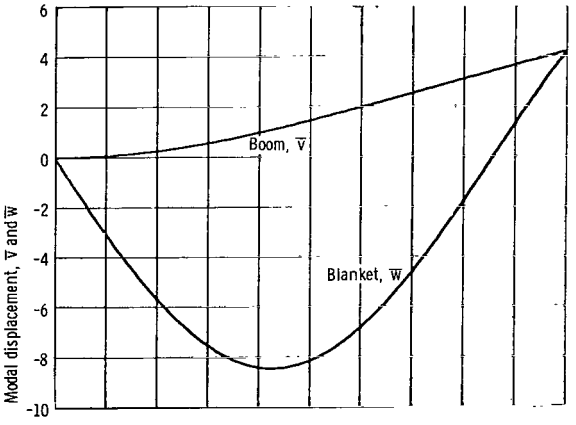

(h) Second bending mode; $P/P_{cr,0} = 0.70$.

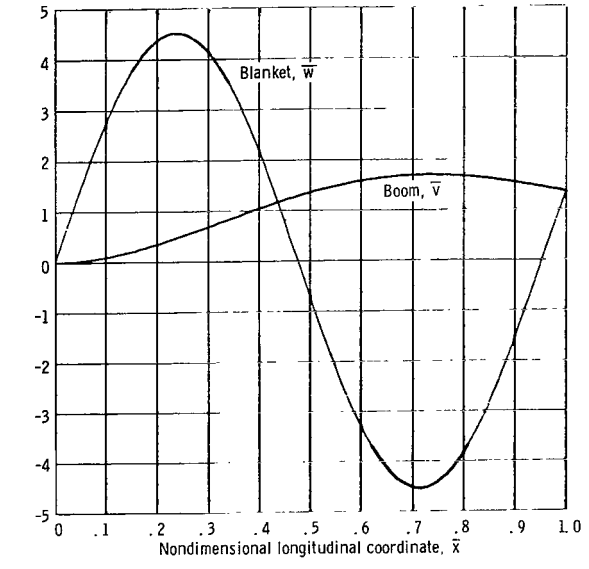

(i) Third bending mode; $P/P_{cr,0} = 0.70$.

Figure 13. - Concluded.

"The aeronautical and space activities of the United States shall be conducted so as to contribute . . . to the expansion of human knowledge of phenomena in the atmosphere and space. The Administration shall provide for the widest practicable and appropriate dissemination of information concerning its activities and the results thereof."

—NATIONAL AERONAUTICS AND SPACE ACT OF 1958

NASA SCIENTIFIC AND TECHNICAL PUBLICATIONS

TECHNICAL REPORTS: Scientific and technical information considered important, complete, and a lasting contribution to existing knowledge.

TECHNICAL NOTES: Information less broad in scope but nevertheless of importance as a contribution to existing knowledge.

TECHNICAL MEMORANDUMS: Information receiving limited distribution because of preliminary data, security classification, or other reasons. Also includes conference proceedings with either limited or unlimited distribution.

CONTRACTOR REPORTS: Scientific and technical information generated under a NASA contract or grant and considered an important contribution to existing knowledge.

TECHNICAL TRANSLATIONS: Information published in a foreign language considered to merit NASA distribution in English.

SPECIAL PUBLICATIONS: Information derived from or of value to NASA activities. Publications include final reports of major projects, monographs, data compilations, handbooks, sourcebooks, and special bibliographies.

TECHNOLOGY UTILIZATION PUBLICATIONS: Information on technology used by NASA that may be of particular interest in commercial and other non-aerospace applications. Publications include Tech Briefs, Technology Utilization Reports and Technology Surveys.

Details on the availability of these publications may be obtained from:

SCIENTIFIC AND TECHNICAL INFORMATION OFFICE

NATIONAL AERONAUTICS AND SPACE ADMINISTRATION

Washington, D.C. 20546